Journal of Chromatography A 1630 (2020) 461509

Contents lists available at ScienceDirect

Journal of Chromatography A

journal homepage: www.elsevier.com/locate/chroma

A sensitive quantitative analysis of abiotically synthesized short homopeptides using ultraperformance liquid chromatography and time-of-flight mass spectrometry

Eric T. Parker[a], Megha Karki[b,1], Daniel P. Glavin[a], Jason P. Dworkin[a,**], Ramanarayanan Krishnamurthy[b,*]

[a] NASA Goddard Space Flight Center, Solar System Exploration Division, 8800 Greenbelt Road, Greenbelt, MD 20771, United States
[b] Department of Chemistry, Scripps Research, 10550 North Torrey Pines Road, La Jolla, CA 92037, United States

ARTICLE INFO

Article history:
Received 5 June 2020
Revised 4 August 2020
Accepted 22 August 2020
Available online 23 August 2020

Keywords:
Homopeptides
Diamidophosphate
Ultraperformance liquid chromatography
Time-of-flight mass spectrometry
Pre-column derivatization

ABSTRACT

In the origins of life field understanding the abiotic polymerization of simple organic monomers (e.g., amino acids) into larger biomolecules (e.g., oligopeptides), remains a seminal challenge. Recently, preliminary observations showed a limited set of peptides formed in the presence of the plausible prebiotic phosphorylating agent, diamidophosphate (DAP), highlighting the need for an analytical tool to critically evaluate the ability of DAP to induce oligomerization of simple organics under aqueous conditions. However, performing accurate and precise, targeted analyses of short oligopeptides remains a distinct challenge in the analytical chemistry field. Here, we developed a new technique to detect and quantitate amino acids and their homopeptides in a single run using ultraperformance liquid chromatography-fluorescence detection/time of flight mass spectrometry. Over an 8-minute retention time window, 18 target analytes were identified and quantitated, 16 of which were chromatographically separated at, or near baseline resolution. Compound identity was confirmed by accurate mass analysis using a 10 ppm mass tolerance window. This method featured limits of detection < 5 nM (< 1 fmol on column) and limits of quantitation (LOQs) <15 nM (< 3 fmol on column). The LODs and LOQs were upwards of ~28x and ~788x lower, respectively, than previous methods for the same analytes, highlighting the quantifiable advantages of this new method. Both detectors provided good quantitative linearity ($R^2 > 0.985$) for all analytes spanning concentration ranges ~3 - 4 orders of magnitude. We performed a series of laboratory experiments to investigate DAP-mediated oligomerization of amino acids and peptides and analyzed experimental products with the new method. DAP readily polymerized amino acids and peptides under a range of simulated environmental conditions. This research underscores the potential of DAP to have generated oligopeptides on the primordial Earth, enhancing prebiotic chemical diversity and complexity at or near the origin of life.

1. Introduction

The primordial Earth likely contained a variety of simple organic compounds (e.g., amino acids), the origins of which, could have included *in situ* synthesis [1-7] and exogenous delivery [8-11]. It has been hypothesized that once present, these monomers could have accumulated in localized environments (e.g., tidal pools) [6] and subsequently undergone processing to generate oligomers [12], ultimately leading to the synthesis of primitive, functional biopolymers.

The prebiotic polymerization of amino acids and the analysis of such mixtures has been a decades-long challenge facing the origin of life field. Numerous previous efforts have been made to address such challenges, with varying degrees of success [13]. Possible prebiotic condensing reagents such as carbonyl sulfide [12], and cyanamide and dicyandiamide [14] have been investigated for their ability to induce the polymerization of amino acids into peptides. These studies have resulted in the successful formation of simple peptides composed of ~2–3 amino acid residues, but larger peptides were consistently difficult to generate. More

* Corresponding author: Department of Chemistry, Scripps Research, 10550 North Torrey Pines Road, La Jolla, CA 92037, USA.
** Co-Corresponding author: NASA Goddard Space Flight Center, Solar System Exploration Division, 8800 Greenbelt Road, Greenbelt, MD 20771, USA.
E-mail addresses: jason.p.dworkin@nasa.gov (J.P. Dworkin), rkrishna@scripps.edu (R. Krishnamurthy).
[1] Present Address: Singular Genomics, 10931 North Torrey Pines Road Suite #100, La Jolla, CA 92037, USA

https://doi.org/10.1016/j.chroma.2020.461509
0021-9673/

recently, Forsythe and Yu et al. [15] explored the co-polymerization of α-amino acids and their chemical cousins, α–hydroxy acids, under wet-dry cycling conditions. This approach demonstrated that larger peptides composed of ~2 – 8 amide bonds could be synthesized. Identifying alternative and complementary prebiotically plausible polymerization pathways, capable of readily generating amino acid oligomers under mild conditions would increase the likelihood of the abiotic emergence of peptides on the early earth under diverse environments.

Diamidophosphate (DAP) is a prebiotically plausible phosphorylating agent that, in the presence of imidazole, can induce the polymerization of phosphates and generate ester bonds between carboxylic acids and alcohols [16,17] in water, at pH 6–8, and under thermally mild (room temperature) conditions. Furthermore, Gibard et al. [17] reported the tentative identification of higher order peptides upon exposing amino acids to imidazole and DAP. These detections were made using ^{1}H NMR and electrospray ionization mass spectrometry (ESI-MS), but the presence of these higher order peptides in a solution comprised of amino acids, imidazole, and DAP affirmed that more rigorous, targeted analytical approaches were needed to comprehensively explore the capability of DAP to oligomerize amino acids.

Diamidophosphate is a very simple compound that could have readily formed on the early Earth via the reaction of prebiotic phosphorus [18] and aqueous ammonia [19,20]. Prebiotically accessible phosphorus could have been delivered by meteorites [21,22], or formed via *in situ* synthesis [23], and significant quantities of dissolved ammonia could have been released into the early Earth's oceans by hydrothermal vents [24]. Furthermore, the geochemical availability of DAP has recently been experimentally demonstrated [25]. Imidazole, which decelerates the condensation and hydrolysis of DAP [17], could have been prebiotically formed via irradiation of atmospheric water, nitrogen, and carbon monoxide or methane [26]. Thus, the reagents necessary to facilitate DAP-mediated polymerization are prebiotically plausible.

Based on the tentative identification of higher order peptides [17] stemming from a mixture of select amino acids, imidazole, and DAP, and given that DAP is a prebiotically plausible compound, we hypothesize that DAP will readily facilitate the formation of peptides composed of Gly, Ala, Asp, Glu, and also oligomerize short peptides (e.g., glycylglycine) under thermally mild, aqueous conditions that are relevant to a prebiotic context. To evaluate this hypothesis, we performed a series of laboratory experiments to determine the effectiveness of DAP to oligomerize amino acids and simple peptides under mild, aqueous conditions. We performed experiments designed to evaluate how changing the molar equivalents of DAP relative to the amino acid in question affected the oligomerization products, using starting reagent concentrations consistent with that which has been used previously in the literature [15,27-28]. We also executed room temperature, mild heating (50 °C), and simulated environmental cycling experiments using lower starting reagent concentrations to evaluate the change in efficacy of the DAP polymerization chemistry with a change in reagent concentrations.

The analyses of the homopeptides generated from these experiments required a robust analytical technique capable of accurately detecting and precisely quantitating oligomers synthesized from the exposure of amino acids and simple peptides to imidazole and DAP. However, the analysis of a mixture of short homopeptides is a formidable analytical challenge. Currently available techniques reported in the literature that target peptides suffer from such drawbacks as long run times [29-32], use of only one detection system [32,33-36], lacking accurate mass analysis [37-39], or detecting a limited number of analytes [40-42]. Forsythe et al. [43] recently implemented a technique capable of detecting a wide range of depsipeptides (mixed amide/ester linkages) based on retention time, drift time, accurate mass, and fragmentation patterns. However, due to limited commercial availability of depsipeptide standards, absolute quantitation was not reported. Ideally, an analytical technique would be developed that provides rapid analysis of a wide range of peptides using multiple detection systems, including accurate mass analysis, and is capable of delivering absolute quantitation of target analytes. Therefore, to facilitate the analysis of oligopeptides generated by laboratory experiments in this work, we developed a new analytical method to detect and quantitate amino acids and associated homopeptides in a single analytical run. The new technique developed here was optimized to address the aforementioned analytical needs. The analytical approach employed here used a combination of ultraperformance liquid chromatography, UV fluorescence detection, and time-of-flight mass spectrometry (UPLC-FD/ToF-MS). Furthermore, because linear oligopeptides were likely readily available to carry out further polymerization chemistry on the primitive Earth *en route* to the formation of the first functional biopolymers, as opposed to diketopiperazines, which are highly stable cyclic dipeptides that could have prevented amino acid residues from being available to engage in further polymerization chemistry [44-46], the method developed here was optimized to target linear homopeptides.

2. Materials and methods

2.1. Chemicals and reagents

All sample handling tools, including glassware, were baked out overnight at 500 °C in air prior to use to remove organic contamination. Millipore Integral 10 ultrapure water (18.2 MΩ-cm, ≤3 ppb total organic carbon) was used for the experiments performed here. All commercially purchased reagents used were acquired from Sigma-Aldrich, Fisher Scientific, Acros Organics, Combi-Blocks, Bachem, Tokyo Chemical Industry, and Waters Corporation. The DAP used in this work was synthesized as described elsewhere [16,47,48]. Stock amino acid and homopeptide solutions were prepared by dissolving individual analyte crystals in ultrapure water. The amino acids and homopeptides used to generate stock solutions were of purities in the 96% - 100% range, and the stock solutions were made to be between 10^{-2} M and 1 M. Once the individual standard solutions of each species were made, they were combined to facilitate the analysis of all target analytes in a single analytical run.

Four reagents were used to enable pre-column derivatization: 1) AccQ·Tag Ultra borate buffer, 2) AccQ·Tag Ultra reagent powder, 3) AccQ·Tag Ultra reagent diluent, and 4) AccQ·Tag derivatization agent**.** Four eluents were used to perform UPLC-FD/ToF-MS analysis: A) AccQ·Tag A buffer, B) AccQ·Tag B buffer, C) strong wash, and D) weak wash. Daily calibrations of the ToF-MS and real-time lock mass corrections were performed using 2 separate solutions. The preparation and implementation of these reagents used for derivatization, analysis, and mass calibration are detailed in §1.1 of the supplementary material.

2.2. Method development

Amino acids and homopeptides were analyzed using a Waters Acquity H–Class UPLC, coupled to a Waters Acquity UPLC FD, and a Waters Xevo G2-XS mass spectrometer. Analyte identification was based on 3 analytical metrics: 1) chromatographic retention time, 2) optical fluorescence, and 3) accurate mass measurement, based on comparison to a mixed standard. The selection of amino acids and homopeptides to analyze in this study was based on a core set of four amino acids. The amino acids Gly, Ala, Asp, and Glu, and their respective homopeptides, were selected for study

because these amino acids: 1) are commonly produced in prebiotic simulation experiments ([1,6–7]), 2) they have been detected in meteorites [49], and 3) they allow for the exploration of how homopeptide synthesis varies between those composed of structurally simple (i.e., Gly and Ala) and more complex (i.e., Asp and Glu) amino acids. In this study, we focused on analyzing the mixture of homopeptides from these amino acids as a demonstration of a proof of concept of analytical capabilities dealing with the first stage complexities at this 'simpler' homopeptide level, before we tackle the long-term issue of how to analyze more complex mixtures involving heteropeptides. Consequently, the targeted homopeptides were diglycine (Gly_2), triglycine (Gly_3), tetraglycine (Gly_4), pentaglycine (Gly_5), hexaglycine (Gly_6), dialanine (Ala_2), trialanine (Ala_3), tetra-alanine (Ala_4), penta-alanine (Ala_5), diaspartic acid (Asp_2), triaspartic acid (Asp_3), tetra-aspartic acid (Asp_4), diglutamic acid (Glu_2), and triglutamic acid (Glu_3). The lengths of homopeptides targeted in this study were dictated by aqueous solubility limits of commercially available analytical standards.

Amino acids and homopeptides underwent pre-column derivatization using Waters AccQ·Tag derivatization agent (6-aminoquinolyl-*N*-hydroxysuccinimidyl carbamate), a fluorophore that enhances analytical specificity by reacting with primary amino groups, and select secondary amino groups [50]. A schematic representing the derivatization reaction is provided in the supplementary material (Figure S1), which illustrates that only the N-terminal primary amino groups of the homopeptides analyzed in this study were successfully derivatized by AccQ·Tag. The AccQ·Tag derivatization agent has the added benefit of being effective in the presence of different salts [50], allowing for the mitigation of otherwise necessary desalting procedures that are sources of sample contamination and loss. This is in contrast to alternative derivatization approaches, such as 9-fluorenylmethyl chloroformate or phenylisothiocyanate [51] and *o*-phthaldialdehyde/*N*-acetyl-L-cysteine [52], which are adversely impacted by the presence of salts or interfering ions. Furthermore, derivatives of AccQ·Tag are stable for at least 1 week at room temperature [50], whereas derivatives of other agents, such as *o*-phthaldialdehyde are often unstable [53]. Consequently, pre-column derivatization was executed by mixing 10 μL of the sample or standard with 70 μL of AccQ·Tag Ultra borate buffer, then adding 20 μL of the AccQ·Tag agent, prior to heating at 55 °C for 10 min. Following derivatization, samples and standards were ready for analysis. Since the AccQ·Tag derivatization agent was the only reagent responsible for derivatizing target analytes, only results from AccQ·Tag derivatization are discussed here.

UPLC separations have been performed using a 2.1 × 150 mm, 1.7 μm Waters Acquity UPLC BEH Phenyl column. Target analytes were eluted using the following gradient: 0 – 9.5 min, 100% eluent A, 9.5 – 16 min, 100 – 92% eluent A, 16 – 20 min, 92 – 82% eluent A, 20 – 21 min, 82 – 100% eluent A, 21 – 25 min, 100% eluent A. The autosampler was maintained at 25 °C, the injection volume was 2 μL, the eluent flow rate was held constant at 0.3 mL min^{-1}, and the column was maintained at 30 °C. The FD was operated with an excitation wavelength of 266 nm and an emission wavelength of 473 nm.

The ToF-MS was equipped with a dual ESI source arrangement, where both ESI sources were operated in positive ion mode. The primary ESI source was used under the following conditions: capillary voltage, 3.5 kV, sampling cone voltage, 40 V, source temperature, 120 °C, desolvation gas temperature, 500 °C, cone gas (N_2) flow, 50 L hr^{-1}, desolvation gas (N_2) flow, 1000 L hr^{-1}. When using the primary ESI source, the ToF-MS was calibrated over the 50 – 1200 *m/z* range. The purpose of implementing the secondary ESI source was to account for the possibility of small deviations in the *m/z* scale after daily calibrations were performed, and thus provide an independent leucine enkephalin standard signal at *m/z* 556.2771. The secondary ESI source was implemented using parameters identical to those when the primary ESI source was utilized, except the secondary ESI source used a capillary voltage of 2.8 kV and a reference cone voltage of 30 V. The ToF-MS analyzer was operated in V-optics mode, which implemented a reflectron to achieve a full width at half maximum resolution of 22,000 based on the *m/z* value of leucine enkephalin. The detector voltage setting was 2225 V, and the *m/z* range over which data were collected was 100 – 1000. A mass tolerance of 10 ppm was implemented for the purpose of accurate mass identification of target analytes by ToF-MS.

Following the completion of analytical development, the qualitative and quantitative performance of the method was comprehensively evaluated by performing analytical figures of merit experiments. The details of these experiments can be found in §1.3 of the supplementary material, and the results from the analytical figures of merit experiments can be found in Section 2.2 of the supplementary material.

2.3. DAP/dry-down experiments

Experimental reaction solutions composed of select amino acids, imidazole, and DAP were prepared for the DAP/dry-down experiments. The objectives of the DAP/dry-down experiments were two-fold: 1) to evaluate how homopeptide synthesis was affected by changing the molar equivalents of DAP relative to the amino acid, and 2) to determine how homopeptide synthesis was affected by either leaving the experimental reaction solutions in the liquid state at room temperature, or bringing the experimental reaction solutions to dryness.

The amino acids chosen for these experiments were Ala, Asp, and Glu. Each individual amino acid was combined with imidazole and DAP in an aqueous solution. In each solution, the amino acid and imidazole were both present at 0.1 M. Each amino acid was exposed to 3 different DAP concentrations in separate solutions, 0.05 M (i.e., 0.5 equivalents), 0.1 M (i.e., 1 equivalent), or 0.2 M (i.e., 2 equivalents). Each solution was stirred at room temperature for 14 days. The pH of each solution was between 8.5 – 9.3 over the course of the 14-day reaction. At the end of 14 days, experimental reaction solutions were designated to either be brought to dryness in a Centrivap centrifugal vacuum dryer, or to be not dried. In addition to these experimental reaction solutions, experimental control solutions were prepared. The experimental control solutions were prepared in an identical fashion as the experimental reaction solutions, except after the 14-day reaction period, the experimental control samples were pH-adjusted between 1.0 – 1.35 and stirred for 16 h to stop the reaction. Subsequently, experimental control solutions were designated to either be brought to dryness in a Centrivap, or to be not dried. The experimental solutions prepared for these experiments and the experimental conditions used are detailed in Table 1. After generation, the experimental solutions underwent a 100x dilution. The purpose of this dilution step was to avoid potentially overwhelming the ToF-MS detector by otherwise exposing the detector to very large concentrations ($\geq$ 1 mM) of the amino acids that existed in the experimental solutions. After dilution, experimental control solutions and experimental reaction solutions were analyzed identically.

2.4. Room temperature/heating experiments

The objectives of the room temperature/heating experiments were two-fold: 1) to evaluate homopeptide synthesis under room temperature (23 ± 3 °C), aqueous conditions, and 2) to determine how homopeptide synthesis was affected by exposing experimental reaction solutions to mild heating at 50 ± 0.6 °C. Individual experimental reaction solutions using all 4 target amino acids, imida-

Table 1
Composition of experimental reaction solutions and experimental conditions used during the execution of the DAP/dry-down experiments.

Amino Acid (M)	DAP (M)	Imidazole (M)	Temperature	pH	Time (days)	Processing
Ala (0.10) Asp (0.10) Glu (0.10)	0.05 0.10 0.20	0.10	Room Temperature	8.5 – 9.3	14	Dried, or Not Dried

Table 2
Composition of experimental reaction solutions and experimental protocol implemented during the execution of the room temperature/heating experiments.

Amino Acid (M)	DAP (M)	Imidazole (M)	Temperature	Sample Collection Frequency
Gly (0.01) Ala (0.01) Asp (0.01) Glu (0.01)	0.01	0.01	Room Temperature, or 50 °C	$t_i = 0$ days $t_1 = 3$ days $t_2 = 6$ days $t_3 = 9$ days $t_4 = 24$ days $t_f = 106$ days

Table 3
Composition of experimental reaction solutions and experimental protocol implemented during the execution of the simulated environmental wet-dry cycling experiments. In this table, DD = dry-down, hrs = hours, No. = number, and RT = room temperature.

Species (M)	DAP (M)	Imidazole (M)	No. of Cycles	Cycle Descriptions
Gly (0.01) Ala (0.01) Asp (0.01) Glu (0.01) Gly_2 (0.01)	0.01	0.01	0 - 4	**0 Cycles:** no DD **1 Cycle:** DD at 50 °C for 24 hrs **2 Cycles:** 1 cycle + rehydrate at RT for 24 hrs + DD at 50 °C for 24 hrs **3 & 4 Cycles:** similar to 2 cycles

zole, and DAP were prepared for these experiments. For each experimental reaction solution, the amino acid, imidazole, and DAP were all equimolar, at a concentration of 10 mM. Experimental reaction solutions were sampled for analysis according to the following frequency: $t_i = 0$ days, $t_1 = 3$ days, $t_2 = 6$ days, $t_3 = 9$ days, $t_4 = 24$ days, and $t_f = 106$ days. Table 2 details the composition and treatment of each experimental reaction solution.

For each experimental reaction solution prepared, a corresponding experimental control solution was prepared. The experimental control solutions were prepared identically to the experimental reaction solutions, except the experimental control solutions were composed of an amino acid and imidazole, but did not include DAP. The purpose of the experimental control solution was to verify that homopeptides did not form in the absence of DAP. After generation, and prior to analysis, the experimental solutions were sampled at their respective times, and underwent 10x dilutions. These dilution steps served the purpose of avoiding potentially overwhelming the ToF-MS detector with very large concentrations of initial reactants.

2.5. Simulated environmental wet-dry cycling experiments

The objectives of the simulated environmental wet-dry cycling experiments were three-fold: 1) to evaluate homopeptide synthesis using starting reagent concentrations 10x less than those used in the DAP/dry-down experiments, 2) to determine how homopeptide synthesis was affected by exposing experimental solutions to multiple dry-down/rehydration cycles, and 3) to determine if DAP is capable of oligomerizing short peptides, in addition to amino acids. Individual experimental reaction solutions using all 4 target amino acids and Gly_2, imidazole, and DAP were prepared for the simulated environmental cycling experiments. For each experimental reaction solution, the amino acid or peptide, imidazole, and DAP were all equimolar, at a concentration of 10 mM. The simulated environmental cycles were performed as described in Table 3. After the completion of each simulated environmental cycle, samples were rehydrated and prepared for analysis as described above prior to analysis by UPLC-FD/ToF-MS. Experimental control solutions were prepared as described in the previous section. Experimental reaction solutions and experimental control solutions were also diluted 10x prior to analysis, as detailed previously. Analyses of samples generated from the simulated environmental wet-dry cycling experiments were performed identically to the analyses of samples generated by the other experiments performed in this work.

3. Results and discussion

3.1. Method development

The analytical technique developed here targeted a suite of 18 analytes composed of amino acids and their respective homopeptides. The chromatographic approach implemented achieved at, or near, baseline resolution for 16 of 18 species (Fig. 1). The only 2 analytes that were not well resolved were Gly_3 and Gly_4. While these compounds coeluted and therefore could not be differentiated by fluorescence, they were detected at different $[M+H]^+$ values and were therefore fully resolved by the mass spectrometer, within a mass accuracy window of 10 ppm. The AccQ·Tag derivatization agent facilitated reversed-phase UPLC separation of hydrophilic amino acids and peptides by covalently bonding a hydrophobic 6-aminoquinolyl carbamate moiety to their respective primary amino groups, which increased the overall hydrophobicity of the target analytes. Given the hydrophobic nature of the stationary phase used in the reversed-phase UPLC technique discussed here, the derivatized target analytes experienced increased interaction with the stationary phase compared to their non-derivatized counterparts. In turn, the AccQ·Tag derivatization agent enabled the enhanced chromatographic retention and separation of otherwise hydrophilic amino acids and peptides using a reversed-phase

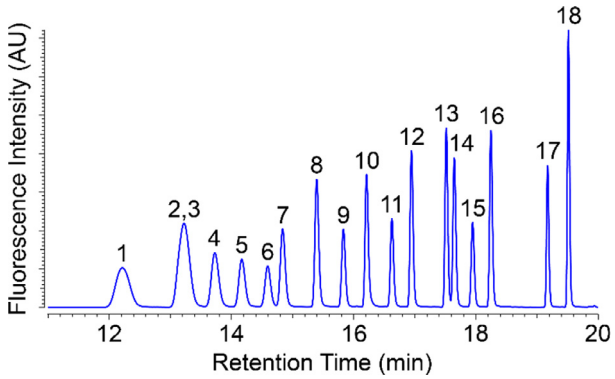

Fig. 1. At, or near, baseline separation was achieved for 16 of the 18 target analytes. The 11 – 20-minute region of a fluorescence chromatogram for a combined standard containing the amino acids and homopeptides targeted in this study, demonstrating the efficacy of the chromatographic technique developed. Peak identification: 1) Gly_2, 2) Gly_3, 3) Gly_4, 4) Gly_5, 5) Gly_6, 6) Gly, 7) Asp_2, 8) Asp_3, 9) Asp, 10) Asp_4, 11) Glu, 12) Glu_2, 13) Glu_3, 14) Ala_2, 15) Ala, 16) Ala_3, 17) Ala_4, 18) Ala_5. Here, AU = arbitrary units and min = minutes. Please see Table S1 for a summary of the detection metrics observed for the method developed here.

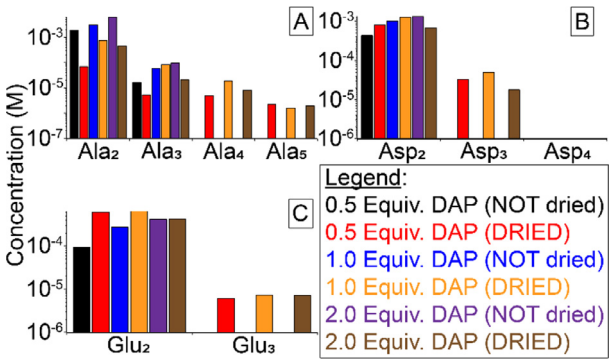

Fig. 2. Results of DAP/dry-down experiments. These experiments were performed using Ala (A), Asp (B), and Glu (C) as the amino acids. The findings demonstrate that longer homopeptides formed when mixtures were dried down as opposed to left as solutions.

UPLC approach. Additional details pertaining to the observed chromatographic results are provided in Section 2.1 of the supplementary material. Furthermore, a breakdown of the detection parameters for each of the target analytes is provided in Table S1.

Reports of analytical methods used for the analysis of short oligopeptides, particularly those applied to prebiotic chemistry research, are unfortunately often not necessarily accompanied by an analytical figures of merit evaluation to rigorously constrain the quantitative performances of the methods [34,54,55]. However, several reports of existing techniques have targeted select short oligopeptides also targeted in the current study, and concomitantly provided quantitative performance characteristics for these methods. For example, You et al. [56] used *N*-hydroxysuccinimidyl-α-(9-phenanthrene)-acetate pre-column derivatization with high performance liquid chromatography (HPLC) and fluorescence spectrophotometry to obtain limit of detection (LOD) values for Gly_2 and Gly_3. Additionally, Zhu et al. [57] used fluorescamine post-column derivatization with capillary electrophoresis and fluorescence detection to obtain LOD values for Gly_2 – Gly_6 oligomers, Ala_2, and Ala_5. Furthermore, Wang et al. [58] used a micro-fluidic chip and laser induced fluorescence detection to obtain an LOD value for Gly_2. Lastly, Campbell et al. [59] recently published limit of quantitation (LOQ) values for a method used to analyze Gly_2 – Gly_6 oligomers by ion-pair HPLC and UV–Vis detection. When comparing LOD values from existing methods to the LOD values (e.g., Table S3) obtained from the method developed in this current work, the technique developed here provided upwards of ~3 – 12x lower LOD values for Gly_2 [56–58], ~4 – 18x lower LOD values for Gly_3 [56,57], and ~4 – 10x lower LOD values for Gly_4 – Gly_6 and ~22 – 28x lower LOD values for Ala_2 and Ala_5 [57]. When comparing LOQ values from an existing method to the LOQ values (e.g., Table S3) obtained from the method developed in the current work, the technique developed here provided upwards of ~119 – 788x lower LOQ values for Gly_2 – Gly_6 [59].

These comparative results underscore the importance of conducting a rigorous analytical figures of merit assessment when reporting the development of a new method, or the application of an existing method. In addition to providing lower LOD and LOQ values for the aforementioned oligopeptides that were concomitantly targeted by existing methods [56–59], the method developed in the current work also detected a more diverse set of oligopeptides than reported in other works focused on the analysis of oligopeptides relevant to origins of life chemistry [60–62]. Overall, it can be concluded that the method developed here provides analytical chemists and prebiotic chemists with a fast, sensitive technique capable of analyzing a wide range of oligopeptides using multiple detectors, including an accurate mass analyzer, without needing to perform off-line desalting that may otherwise contribute to sample contamination and loss.

3.2. DAP/dry-down experiments

The results of the experimental reaction samples being subjected to the DAP/dry-down experiments are given in Fig. 2. The formation of dimers and trimers of Ala (Fig. 2A), and dimers of Asp (Fig. 2B) and Glu (Fig. 2C) were comparable between dried and non-dried samples. The experimental control samples (pH adjusted to 1.0 – 1.35 after the 14-day reaction) failed to match the homopeptide synthetic capabilities of the experimental reaction samples (not pH adjusted). This is consistent with the expectation that acidifying the experimental control samples would quench the polymerization reaction due to the hydrolysis of DAP (pKa ≈ 5) under these conditions [63].

Based on the results shown in Fig. 2, it is clear that homopeptide elongation is greatest when solutions composed of an amino acid, imidazole, and DAP are dried down. This is consistent with previous publications, which have indicated that dehydration is a critical step for the polymerization of monomers [64,65]. What can also be deduced from Fig. 2 is that dried experimental reaction solutions that contained 1 equivalent of DAP relative to the amino acid, generally produced higher abundances of longer homopeptides. This information was used to design the subsequent oligomerization experiments.

Subjecting a solution containing 0.1 M Ala + 0.1 M imidazole + 0.1 M DAP to a dry-down resulted in the formation of the following concentrations (% yields) of homopeptides: ~751 μM (0.75%) Ala_2, ~84 μM (0.08%) Ala_3, ~19 μM (0.02%) Ala_4, and ~2 μM (0.002%) Ala_5 (Fig. 2A). Subjecting a solution containing 0.1 M Asp + 0.1 M imidazole + 0.1 M DAP to a dry-down resulted in the formation of the following concentrations (% yields) of homopeptides: ~1 mM (1.3%) Asp_2, ~50 μM (0.05%) Asp_3, and Asp_4 was below the instrumental LOD (Fig. 2B). Likewise, bringing the experimental reaction solution composed of 0.1 M Glu + 0.1 M imidazole + 0.1 M DAP to dryness resulted in the following concentrations (% yields) of homopeptides: ~654 μM (0.7%) Glu_2 and ~7 μM (0.007%) Glu_3 (Fig. 2C). The % yields of homopeptides produced during the DAP/dry-down experiments are similar to those observed in other dehydration-based oligomerization chemistries [66,67].

Table 4
Homopeptide yields from room temperature/heating experiments. This table summarizes: 1) the maximum homopeptide syntheses that occurred within each solution subjected to room temperature, or mild heating (50 °C) conditions, 2) the respective yields of these homopeptides synthesized based on the t_i concentration (10 mM) of the amino acids being evaluated, and 3) the time point at which the maximum homopeptide syntheses were observed. In this table, I = imidazole and RT = room temperature. Uncertainties (δ_x) were determined as the standard error ($\delta_x = \sigma_x \cdot (n)^{-1/2}$), whereby the uncertainties were based on the standard deviation (σ_x) of the average value of triplicate measurements ($n = 3$).

Solution (Temperature)	Product	Concentration (μM)	Yield (%)	Time (Days)
Gly + I + DAP (RT)	Gly_2 Gly_3	83.0 ± 2.1 +	0.83 ◇	106 106
Gly + I + DAP (50 °C)	Gly_2 Gly_3	120.7 ± 7.5 +	1.21 ◇	106 106
Ala + I + DAP (RT)	Ala_2 Ala_3	76.7 ± 3.4 +	0.77 ◇	106 106
Ala + I + DAP (50 °C)	Ala_2 Ala_3	39.6 ± 1.2 +	0.40 ◇	106 106
Asp + I + DAP (RT)	Asp_2	77.5 ± 2.7	0.78	24
Asp + I + DAP (50 °C)	Asp_2	50.2 ± 5.1	0.50	9
Glu + I + DAP (RT)	Glu_2	2.1 ± 0.4	0.02	106
Glu + I + DAP (50 °C)	Glu_2	+	◇	24

+ Analyte was detected in the 10x diluted experimental reaction solutions that were analyzed, but concentrations did not exceed the LOQ.
◇ Yields are not reported because the analyte concentrations in the analyzed 10x diluted experimental reaction solutions, were below the LOQ.

3.3. Room temperature/heating experiments

The room temperature/heating experiments offer a glimpse into the DAP-mediated amino acid oligomerization chemistry at relatively low (room) temperature conditions, and also under thermally mild (50 °C) conditions. For the purpose of demonstrating the efficacy of DAP-mediated homopeptide synthesis, experimental data from the oligomerization of Gly to form Gly_2 is detailed here, while experimental data from the oligomerization of Gly to form Gly_3, and the oligomerizations of the other three amino acids considered (Ala, Asp, and Glu) are detailed in Section 2.3 of the supplementary material.

Maximum Gly_2 formation under room temperature and mild heating conditions was observed after 106 days (Table 4). By examining Gly_2 accurate mass chromatograms after 106 days, it can be seen that the magnitude of the Gly_2 signal is slightly greater in the 50 °C experimental reaction solution composed of Gly, imidazole, and DAP, than it is for the same experimental reaction solution kept at room temperature (Fig. 3A). It can also be seen that in the absence of DAP, Gly_2 is not formed, demonstrating that the presence of DAP is essential to enable oligomerization. Experimental reaction solutions generated detectable quantities of Gly_2 by the first collection time point ($t_1 = 3$ days) when exposed to mild heating (50 °C), whereas experimental reaction solutions left at room temperature did not generate detectable quantities of Gly_2 until the second collection time point ($t_2 = 6$ days). At the end of the 106-day experiment, the heated experimental reaction solutions contained ~45% more Gly_2 than did the experimental reaction solutions left at room temperature (Fig. 3B).

The homopeptide yields observed from the room temperature and heating experiments are overviewed in Table 4, and are similar to those observed elsewhere [66,67]. It is worth noting that during the room temperature experiments, the simple amino acids, Gly and Ala, were able to form dimer and trimer homopeptides; however, the more complex amino acids, Asp and Glu, could only form dimers. Furthermore, neither Gly nor Ala were able to facilitate the synthesis of tetramers or longer species. This is in contrast to the solutions that were brought to dryness during the DAP/drydown experiments, which readily formed larger homopeptides, illustrating the importance of dehydration to drive amino acid polymerization. It should be pointed out that over the course of the room temperature/heating experiments, it was observed that the application of mild heating only made a noteworthy impact to the oligomerization of simple amino acids. Under both room temperature and mild heating conditions, the overall amino acid polymerization efficiency, in terms of total homopeptide yields, was identical: Gly > Asp > Ala >> Glu. Additionally, the overall amino acid polymerization efficiency, in terms of homopeptide length was also identical for both room temperature and mild heating conditions: Gly = Ala > Asp = Glu. The observed homopeptide synthetic discrepancies between simple and complex amino acids may likely be due to the relative structural complexity of Asp and Glu resulting in the formation of decreased homopeptide chain lengths in the absence of dehydration.

From the room temperature/heating experiments, three conclusions can be made: 1) DAP is readily capable of inducing the oligomerization of amino acids under thermally mild, aqueous conditions, thus indicating that elevated temperatures are not required to oligomerize amino acids in the presence of DAP and imidazole, 2) DAP can oligomerize both simple and relatively complex amino acids, and 3) application of mild heating does not necessarily result in an increased yield of oligomers for all amino acids tested.

3.4. Simulated environmental wet-dry cycling experiments

For the purpose of evaluating DAP-mediated homopeptide synthesis when subjected to multiple simulated environmental wet-dry cycles, experimental data from the oligomerizations of all 4 amino acids are detailed here. Experimental data from the oligomerization of short peptides (Gly_2) are detailed in Section 2.4 of the supplementary material.

Amino acid-based homopeptide syntheses observed in the experimental reaction solutions is demonstrated in Fig. 4. Homopeptides were not detectable in experimental reaction solutions that

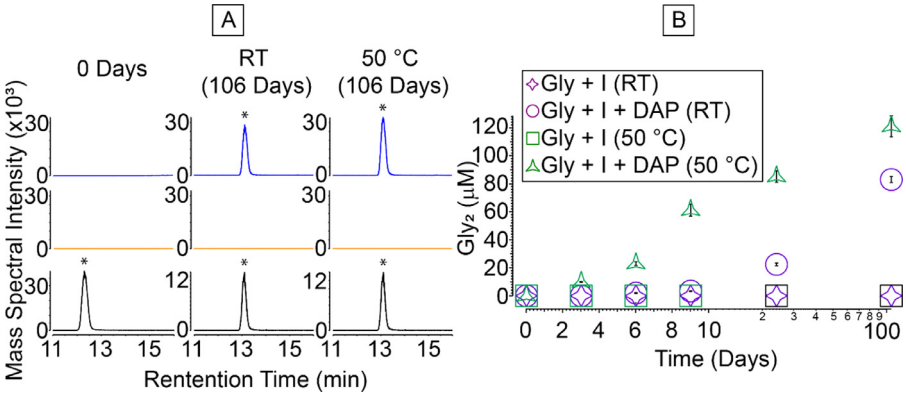

Fig. 3. Gly_2 production under room temperature and mild heating conditions. A) Accurate mass chromatograms of a Gly_2 standard (bottom, black), reaction mixture of a solution of Gly + imidazole (middle, orange), and reaction mixture of a solution of Gly + imidazole + DAP (top, blue). Data are collected after 0 days (t_i) and after 106 days (t_f), when maximum Gly_2 concentrations were reached for both room temperature and mild heating (50 °C) experimental reaction solutions. Accurate mass chromatograms were extracted from *m/z* 303.1093. Asterisks denote peaks that represent Gly_2. B) Gly_2 is not synthesized in the absence of DAP, and Gly_2 synthesis is consistently enhanced when mild heating is applied to the experimental reaction solutions, compared to room temperature conditions. Samples portrayed here were analyzed in triplicate. Uncertainties (δ_x) were determined as the standard error ($\delta_x = \sigma_x \cdot (n)^{-1/2}$), whereby the uncertainties were based on the standard deviation (σ_x) of the average value of 3 separate measurements ($n = 3$). Here, *I* = imidazole, min = minutes, and RT = room temperature.

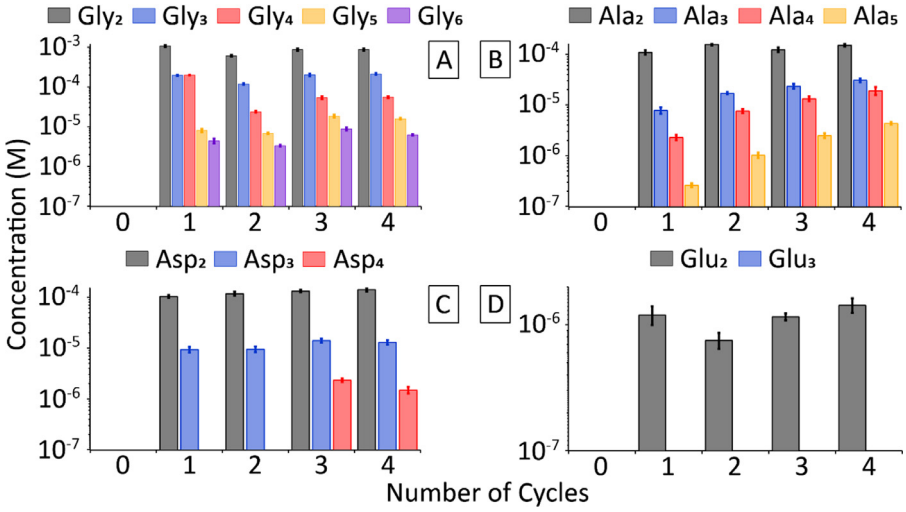

Fig. 4. Amino acid-based homopeptide production as a function of simulated environmental wet-dry cycling. Gly_2 – Gly_6 homopeptides were synthesized after just 1 cycle, and were consistently present with each additional cycle (A). Ala_2 – Ala_5 homopeptides were synthesized after just 1 cycle and were consistently present with each additional cycle (B). Asp_2 and Asp_3 homopeptides were synthesized after 1 cycle; however, it was not until a third simulated environmental cycle was performed that Asp_4 was synthesized (C). Glu_2 was synthesized after 1 cycle; however, Glu_3 was not synthesized over the course of the simulated environmental wet-dry cycling experiments (D). Samples portrayed here were analyzed in triplicate. Uncertainties (δ_x) were determined as the standard error ($\delta_x = \sigma_x \cdot (n)^{-1/2}$), whereby the uncertainties were based on the standard deviation (σ_x) of the average value of 3 separate measurements ($n = 3$).

had not undergone simulated environmental cycling. Experimental control solutions failed to produce homopeptides, while experimental reaction solutions readily synthesized homopeptides. Gly-based homopeptides, up to Gly_6, were promptly generated by wet-dry cycling; however, Gly-based homopeptide abundances were not significantly impacted by exposure to multiple simulated environmental wet-dry cycles, except for Gly_4 abundance, which dropped noticeably after exposure to a second cycle (Fig. 4A). Ala-based homopeptides, up to Ala_5, were generated after 1 wet-dry cycle, and Ala_5 abundances gradually increased with increased cycling, while other Ala-based homopeptide abundances varied to a lesser extent (Fig. 4B). Asp- and Glu-based homopeptides were generated less readily than Gly- or Ala-based homopeptides. Asp_2 and Asp_3 homopeptides were produced after 1 simulated environmental wet-dry cycle; however, Asp_4 did not occur until 3 simulated environmental wet-dry cycles had been performed. (Fig. 4C) Once formed, Asp-based homopeptide abundances did not vary significantly when subjected to additional simulated environmental wet-dry cycles. Glu_2 was synthesized after 1 simulated environmental wet-dry cycle (Fig. 4D), albeit at relatively low abundances (~1 μM) (Table 5). Glu_2 was consistently present in the experimental reaction solutions with each additional simulated environmental cycle; however, Glu_3 was not synthesized at detectable quantities after 4 simulated environmental wet-dry cycles.

The homopeptide yields observed from simulated environmental cycling experiments are overviewed in Table 5. The order of combined homopeptide yields from their respective starting reagents during the simulated environmental wet-dry cycling experiments was Gly_2 > Gly > Ala > Asp >> Glu. Interestingly, subjecting a 10 mM equimolar solution of Gly_2, imidazole, and DAP to simulated environmental cycling resulted in a combined Gly_2 oligomer yield of >18%, including a 15% yield of Gly_4. This is in contrast to a combined Gly oligomer yield of ~15%, including a <2% yield of Gly_4 from a solution containing 10 mM each of Gly, imidazole, and DAP. The observed greater efficiency of oligomerizing a small peptide is consistent with the report that amino acid

Table 5
Homopeptide yields from simulated environmental cycling experiments. This table summarizes: 1) the maximum homopeptide syntheses that occurred within each solution exposed to simulated environmental cycling experiments, 2) the respective yields of these homopeptides synthesized based on the t_i concentration (10 mM) of the amino-based compound being evaluated, and 3) the cycle number at which the maximum homopeptide syntheses were observed. In this table, I = imidazole, RT = room temperature, No. = Number, and N/A = not applicable. Uncertainties (δ_x) were determined as the standard error ($\delta_x = \sigma_x \cdot (n)^{-1/2}$), whereby the uncertainties were based on the standard deviation (σ_x) of the average value of triplicate measurements ($n = 3$).

Solution	Product	Concentration (μM)	Yield (%)	Cycle No.
Gly + I + DAP	Gly_2	1065.1 ± 48.3	10.7	1
	Gly_3	212.0 ± 10.1	2.12	4
	Gly_4	197.6 ± 3.5	1.98	1
	Gly_5	18.3 ± 1.4	0.18	3
	Gly_6	8.8 ± 0.7	0.09	3
Ala + I + DAP	Ala_2	155.8 ± 6.6	1.56	2
	Ala_3	30.7 ± 2.5	0.31	4
	Ala_4	19.1 ± 3.4	0.19	4
	Ala_5	4.3 ± 0.3	0.04	4
Asp + I + DAP	Asp_2	142.0 ± 11.1	1.42	4
	Asp_3	14.1 ± 1.2	0.14	3
	Asp_4	2.3 ± 0.2	0.02	3
Glu + I + DAP	Glu_2	1.4 ± 0.2	0.01	4
	Glu_3	<0.02	N/A	N/A
Gly_2 + I + DAP	Gly_4	1496.0 ± 379.4	15.0	4
	Gly_6	362.5 ± 38.8	3.63	4

monomers are more difficult to condense than two small peptides of at least dipeptide size [64]. Furthermore, this result indicates that DAP shows promise as an agent capable of oligomerizing polymerized species, with one implication being that DAP may be able to convert linear dipeptides into linear tetrapeptides, thereby helping to limit the formation of highly stable diketopiperazines [68–70] that would otherwise act as an amino acid thermodynamic sink, which hinders further polymerization chemistry [44–46].

The yields of homopeptides synthesized from amino acids in the simulated environmental wet-dry cycling experiments all exceed those observed in the room temperature/heating experiments, except for Glu-based homopeptides. In the simulated environmental wet-dry cycling experiments, the Glu-based homopeptide yield (0.01%) was comparable to that observed in the room temperature experiments (0.02%). These results affirm that for most amino acids, dehydration instituted by simulated environmental wet-dry cycling is critical to generating longer chain lengths, and abundances, of homopeptides. The caveat in this case being Glu, which generally struggles to oligomerize with itself, possibly due to its relatively complex structure. It is also possible that Glu oligomerization yields pyroglutamic acid, a 5-membered gamma-lactam structure [71] by the attack of the alpha-amino group onto the gamma-carboxylic acid that has been activated by DAP. Alternatively, Glu oligomerization could be hindered by the formation of Glu diketopiperazine, the thermodynamic end-product of Glu oligomerization [72–74].

When comparing the results of the simulated environmental wet-dry cycling experiments to those of the DAP/dry-down experiments (Fig. 2), two stark contrasts exist: 1) the difference in Asp-based homopeptide synthesis and 2) the difference in Glu-based homopeptide synthesis. The DAP/dry-down experiments demonstrated that Asp_4 was not synthesized after 1 dry-down, yet the simulated environmental wet-dry cycling experiments showed that Asp_4 was generated, but multiple wet-dry cycles were required to do so (Fig. 4C). The need for additional cycling to form larger Asp-based homopeptides, may be due to the structural complexity of Asp hindering oligomerization. Additionally, the DAP/dry-down experiments indicated that Glu_3 was formed after 1 dry-down event when 0.1 M Glu was exposed to equimolar quantities of imidazole and DAP (Fig. 2). However, the simulated environmental wet-dry cycling experiments indicated that when the starting reagent concentrations were dropped by 1 order of magnitude, Glu_3 could not be formed, even after exposure to 4 wet-dry cycles. It is likely this observed lack of oligomerization efficiency was a direct result of the reduction in starting Glu concentration used in the simulated environmental wet-dry cycling experiments, compared to those used in the DAP/dry-down experiments.

The impact that the starting reagent concentration has on the efficacy of a given polymerization chemistry being studied is critical to constraining the prebiotic plausibility of the oligomerization reaction in question. In the case of possible primitive amino acid polymerization reactions, the current prebiotic chemistry literature does not provide experimental evidence demonstrating that relatively large concentrations of amino acid starting reagents were likely to have accumulated under simulated primordial Earth environments. In contrast, the prebiotic chemistry literature suggests that considering the world's oceans travel through the hydrothermal vents every 10 million years [75], amino acid concentrations in the primitive oceans likely did not surpass 300 μM [76]. However, localized environments, such as tidal lagoons or eutectic ponds are thought to have possibly been more impactful for primordial chemical evolution [77,78] because organic species may have accumulated to larger concentrations in these types of environments [79]. Yet, prebiotically plausible concentrations that amino acids could have accumulated to in these localized environments remain poorly understood.

One potential way to help improve the understanding of the accumulation of larger concentrations of amino acids in localized environments on the early Earth is to attempt to quantitatively constrain amino acid precursor concentrations in these types of environments. Toner and Catling [80] recently examined possible prebiotic concentration mechanisms for cyanide, which is an integral reagent in the Strecker synthesis of amino acids. In this work, Toner and Catling [80] used an aqueous model based on experimental data to provide a quantitative estimate of cyanide concentrations reached in sodium bicarbonate-rich, closed-basin lakes, which may have served as a prebiotic environment in which cyanides could have accumulated in the presence of evaporation and inflowing water. It was determined that in such a closed-lake basin, cyanide, in the form of ferrocyanide could reach concentrations as high as 700 mM when atmospheric CO_2 partial pressures were relatively low and atmospheric HCN partial pressures were relatively high, but that cyanide abundances would dip to the micromolar concentration range if the converse atmospheric conditions were present [80]. While these results are pertinent to prebiotic amino acid concentrations, it remains uncertain to what extent these cyanide concentrations would have necessarily contributed to the synthesis of amino acids in such an environment, and how subsequent peptide syntheses would be affected. This points to an important limitation in the current origin of life literature, which is that the possible primordial concentrations of amino acids in localized environments are poorly understood because these concentration estimates depend on the abundances of precursors and the volumes of solvents in such microenvironments, both of which are also not necessarily well-constrained. Thus, further work is needed to better understand if wet-dry cycle-induced peptide synthesis experiments reported in the literature that use relatively high starting concentrations of organic monomers, constitute a geochemically plausible prebiotic polypeptide synthetic pathway.

The comparative results in this work shed light on how reducing the starting concentration of an amino acid reduces the efficiency of the studied polymerization chemistry. In turn, such a reduction in polymerization efficiency can impact the prebiotic

plausibility of the polymerization chemistry in question. Therefore, it can be concluded that future explorations pertaining to possible prebiotic polypeptide synthetic chemistries should be evaluated using lower starting reagent concentrations that are more likely to be prebiotically plausible.

4. Conclusions

The research presented here entailed the development of a new analytical technique necessary to evaluate the capability of a plausible prebiotic phosphorylating agent, DAP, to induce the oligomerization of amino acids and simple peptides into homopeptides that could have helped set the stage for the chemistries important for life on the early Earth. The new UPLC-FD/ToF-MS method was optimized to be fast, sensitive, and selective, capable of detecting and quantitating a suite of amino acids and associated homopeptides. At, or near, baseline resolution was achieved for 16 of the 18 target analytes by employing AccQ·Tag pre-column derivatization to increase analytical specificity for primary amino groups. Target analyte identification was confirmed by accurate mass analysis using a mass tolerance of 10 ppm. This new method provided quantitative advantages over existing methods. When compared to previous techniques that targeted identical short homopeptides to those in this study, the new analytical capability developed here was found to provide LOD values upwards of >1 order of magnitude lower [56–58] and LOQ values upwards of 2 – 3 orders of magnitude lower [59]. Both the FD and ToF-MS responded very linearly ($R^2 > 0.985$) to all analytes over a concentration range of ~3 - 4 orders of magnitude.

A series of laboratory experiments were performed to ascertain the effectiveness of DAP at inducing oligomerization, and the experimental samples were analyzed with the newly developed technique. The results of these laboratory experiments demonstrated that DAP readily facilitated the oligomerization of amino acids and simple peptides under mild thermal conditions, in aqueous solutions. The polymerization chemistry also worked at reduced starting reagent concentrations, but the efficiency of the reaction was decreased. This underscores a potential limitation of the oligomerization reaction at even lower starting reagent abundances, similar to those reported for possible geochemical scenarios [76,81]. The results of the laboratory experiments performed here were products of single executions of each experiment, followed by replicate measurements of the samples generated by these experiments. Uncertainty estimates associated with these replicate measurements were calculated as the standard errors of the means, and provide quantitative constraints on the accuracy and precision of the method developed here.

The primary implications of this work are: 1) DAP is a prebiotically plausible phosphorylating agent that could have helped facilitate the chemical evolution necessary to bridge the gap between simple organic molecules and more complex biomolecules with greater biological functionality at, or near, the time of the origin of life, and 2) the new analytical technique developed here is broadly applicable to a wide variety of disciplines that need an analytical capability to detect and quantitate short peptides. Examples of research fields and topics that fall within this category include pharmaceutical drug discovery [82,83], metabolomics of liver disease [84,85], antioxidant properties of food chemistries [86–89], and various agricultural disciplines [36,37]. Perhaps the most exciting implication of this newly developed method for the origin of life field, is its potential for application to investigate peptides in complex, natural samples, including carbonaceous meteorites. Peptides remain a vastly understudied class of soluble organic compounds in meteorites [90], largely due to analytical limitations that previously precluded effectively targeting these species.

The results of this study highlight the need for further exploration into the ability of DAP to facilitate the oligomerization of a mixture of amino acids that would generate heteropeptides. Given the chemical diversity observed in meteorites [91], it is likely that if peptides were formed on meteorite parent bodies, heteropeptides were among those synthesized. The method developed in this current work was optimized for the analysis of homopeptides and therefore the chromatographic gradient of this method may not be able to sufficiently chromatographically resolve a wide array of heteropeptides in its current form. However, the method developed here could be adapted and modified to facilitate the chromatographic resolution and analysis of heteropeptides generated from a mixture of meteoritic amino acids. Additionally, the findings of this exploration underscore the importance of investigating the ability of DAP to enable the synthesis of homochiral peptides from a suite of chiral amino acids with small L-enantiomeric excesses, which could hold significant implications for understanding the origin of homochirality. Lastly, given the presence of the phosphorus-bearing mineral schreibersite in meteorites [21], and the detection of meteoritic ammonia [92], the necessary precursors for DAP formation likely could have existed on meteorite parent bodies to facilitate the formation of DAP. Therefore, DAP should be searched for in meteorites to further evaluate the plausibility of DAP-mediated amino acid oligomerization in extraterrestrial environments.

Declaration of Competing Interest

The authors declare that they have no known competing financial interests or personal relationships that could have appeared to influence the work reported in this paper.

CRediT authorship contribution statement

Eric T. Parker: Methodology, Validation, Formal analysis, Investigation, Resources, Data curation, Writing - original draft, Writing - review & editing, Visualization. **Megha Karki:** Investigation, Resources, Writing - review & editing, Visualization. **Daniel P. Glavin:** Resources, Data curation, Writing - review & editing, Visualization, Supervision, Project administration. **Jason P. Dworkin:** Conceptualization, Methodology, Validation, Formal analysis, Resources, Data curation, Writing - review & editing, Visualization, Supervision, Project administration, Funding acquisition. **Ramanarayanan Krishnamurthy:** Conceptualization, Methodology, Validation, Formal analysis, Resources, Data curation, Writing - review & editing, Visualization, Supervision, Project administration, Funding acquisition.

Acknowledgements

Funding: This work was supported by the Simons Collaboration on the Origin of Life (SCOL) [grant number 302497 issued to Dr. Jason P. Dworkin, and grant number 327124 issued to Prof. Ramanarayanan Krishnamurthy].

Supplementary materials

Supplementary material associated with this article can be found, in the online version, at doi:10.1016/j.chroma.2020.461509.

References

[1] S.L. Miller, A Production of Amino Acids Under Possible Primitive Earth Conditions, Science 117 (1953) 528–529.
[2] S.L. Miller, Production of Some Organic Compounds under Possible Primitive Earth Conditions, J. of the Am. Chem. Soc. 77 (1955) 2351–2361.
[3] D. Ring, Y. Wolman, N. Friedman, S.L. Miller, Prebiotic Synthesis of Hydrophobic and Protein Amino Acids, Proc. of the Natl. Acad. of Sci. U.S.A. 69 (1972) 765–768.

[4] S. Miyakawa, H. Yamanashi, K. Kobayashi, H.J. Cleaves, S.L. Miller, Prebiotic synthesis from CO atmospheres: Implications for the origins of life, Proc. of the Natl. Acad. of Sci. U.S.A. 99 (2002) 14628–14631.

[5] H.J. Cleaves, J.H. Chalmers, A. Lazcano, S.L. Miller, J.L. Bada, A reassessment of prebiotic organic synthesis in neutral planetary atmospheres, Orig. of Life and Evol. of Biosph 38 (2008) 105–115.

[6] A.P. Johnson, H.J. Cleaves, J.P. Dworkin, D.P. Glavin, A. Lazcano, J.L. Bada, The Miller Volcanic Spark Discharge Experiment, Science 322 (2008) 404.

[7] E.T. Parker, H.J. Cleaves, J.P. Dworkin, D.P. Glavin, M. Callahan, A. Aubrey, A. Lazcano, J.L. Bada, Primordial synthesis of amines and amino acids in a 1958 Miller H_2S-rich spark discharge experiment, Proc. of the Natl. Acad. of Sci. U.S.A. 108 (2011) 5526–5531.

[8] J. Oró, Comets and the Formation of Biochemical Compounds on the Primitive Earth, Nature 190 (1961) 389–390.

[9] K. Kvenvolden, J. Lawless, K. Pering, E. Peterson, J. Flores, C. Ponnamperuma, I.R. Kaplan, C. Moore, Evidence for Extraterrestrial Amino-Acids and Hydrocarbons in the Murchison Meteorite, Nature 228 (1970) 923–926.

[10] S. Pizzarello, G.W. Cooper, G.J. Flynn, The Nature and Distribution of the Organic Material in Carbonaceous Chondrites and Interplanetary Dust Particles, in: D.S. Lauretta, H.Y. McSween Jr. (Eds.), Meteorites and the Early Solar System II, The University of Arizona Press, Tucson, Arizona, U.S.A., 2006, pp. 625–651.

[11] D.P. Glavin, C.M.O'D Alexander, J.C. Aponte, J.P. Dworkin, J.E. Elsila, H. Yabuta, The Origin and Evolution of Organic Matter in Carbonaceous Chondrites and Links to Their Parent Bodies, in: N. Abreu (Ed.), Primitive Meteorites and Asteroids, Elsevier, Amsterdam, Netherlands, 2018, pp. 205–271.

[12] L. Leman, L. Orgel, M.R. Ghadiri, Carbonyl Sulfide-Mediated Prebiotic Formation of Peptides, Science 306 (2004) 283–286.

[13] M. Frenkel-Pinter, M. Samanta, G. Ashkenasy, L.J. Leman, Prebiotic Peptides: Molecular Hubs in the Origin of Life, Chem. Rev. 120 (2020) 4707–4765.

[14] E.T. Parker, M. Zhou, A.S. Burton, D.P. Glavin, J.P. Dworkin, R. Krishnamurthy, F.M. Fernández, J.L. Bada, A Plausible Simultaneous Synthesis of Amino Acids and Simple Peptides on the Primordial Earth, Angew. Chem. Int. Ed. 53 (2014) 8132–8136.

[15] J.G. Forsythe, S.-S. Yu, I. Mamajanov, M.A. Grover, R. Krishnamurthy, F.M. Fernández, N.V. Hud, Ester-Mediated Amide Bond Formation Driven by Wet-Dry Cycles: A Possible Path to Polypeptides on the Prebiotic Earth, Angew. Chem. Int. Ed. 54 (2015) 9871–9875.

[16] R. Krishnamurthy, S. Guntha, A. Eschenmoser, Regioselective α-Phosphorylation of Aldoses in Aqueous Solution, Angew. Chem. Int. Ed. 39 (2000) 2281–2285.

[17] C. Gibard, S. Bhowmik, M. Karki, E.-K. Kim, R. Krishnamurthy, Phosphorylation, oligomerization and self-assembly in water under potential prebiotic conditions, Nature Chem 10 (2018) 212–217.

[18] Y. Yamagata, H. Watanabe, M. Saitoh, T. Namba, Volcanic production of polyphosphates and its relevance to prebiotic evolution, Nature 352 (1991) 516–519.

[19] W. Feldmann, E. Thilo, Zur Chemie der kondensierten Phosphate und Arsenate. XXXVIII. Amidotriphosphat, Z. für Anorg. und Allg. Chem. 328 (1964) 113–126.

[20] E. Thilo, The Structural Chemistry of Condensed Inorganic Phosphates, Angew. Chem. Int. Ed. 4 (1965) 1061–1071.

[21] M.A. Pasek, D.S. Lauretta, Aqueous Corrosion of Phosphide Minerals from Iron Meteorites: A Highly Reactive Source of Prebiotic Phosphorus on the Surface of the Early Earth, Astrobiology 5 (2005) 515–535.

[22] M.A. Pasek, J.P. Dworkin, D.S. Lauretta, A radical pathway for organic phosphorylation during schreibersite corrosion with implications for the origin of life, Geochim. et Cosmochim. Acta 71 (2007) 1581–1596.

[23] A.M. Turner, A. Bergantini, M.J. Abplanalp, C. Zhu, S. Góbi, B.-J. Sun, K.-H. Chao, A.H.H. Chang, C. Meinert, R.I. Kaiser, An interstellar synthesis of phosphorus oxoacids, Nature Commun 9 (2018) 3851, doi:10.1038/s41467-018-06415-7.

[24] O. Müntener, Serpentine and serpentinization: A link between planet formation and life, Geology 38 (2010) 959–960.

[25] C. Gibard, I.B. Gorrell, E.I. Jiménez, T.P. Kee, M.A. Pasek, R. Krishnamurthy, Geochemical Sources and Availability of Amidophosphates on the Early Earth, Angew. Chem. Int. Ed. 58 (2019) 8151–8155.

[26] K. Kobayashi, M. Tsuchiya, T. Oshima, H. Yanagawa, Abiotic synthesis of amino acids and imidazole by proton irradiation of simulated primitive earth atmospheres, Orig. of Life and Evol. of Biosph. 20 (1990) 99–109.

[27] S.-S. Yu, M.D. Solano, M.K. Blanchard, M.T. Soper-Hopper, R. Krishnamurthy, F.M. Fernández, N.V. Hud, F.J. Schork, M.A. Grover, Elongation of Model Prebiotic Proto-Peptides by Continuous Monomer Feeding, Macromolecules 50 (2017) 9286–9294.

[28] A.D. McKee, M. Solano, A. Saydjari, C.J. Bennett, N.V. Hud, T.M Orlando, A Possible Path to Prebiotic Peptides Involving Silica and Hydroxy Acid-Mediated Amide Bond Formation, Chembiochem 19 (2018) 1913–1917.

[29] K. Kawamura, M. Shimahashi, One-step formation of oligopeptide-like molecules from Glu and Asp in hydrothermal environments, Naturwissenschaften 95 (2008) 449–454.

[30] N. Xiao, B. Yu, Separation of fluorinated amino acids and oligopeptides from their non-fluorinated counterparts using high-performance liquid chromatography, J. of Fluor. Chem 131 (2010) 439–445.

[31] H. Zhang, Q. Liu, L.J. Zimmerman, A.-J.L. Ham, R.J.C. Slebos, J. Rahman, T. Kikuchi, P.P. Massion, D.P. Carbone, D. Billheimer, D.C. Liebler, Methods for Peptide and Protein Quantitation by Liquid Chromatography-Multiple Reaction Monitoring Mass Spectrometry, Mol. & Cell. Proteom 10 (2011), doi:10.1074/mcp.M110.006593.

[32] F. Zhao, N. Ye, X. Qiu, J. Qian, D. Wang, W. Yue, Z. Zuo, M. Chen, Identification and comparison of oligopeptides during withering process of White tea by ultra-high pressure liquid chromatography coupled with quadrupole-orbitrap ultra-high resolution mass spectrometry, Food Res. Int. 121 (2019) 825–834.

[33] M. Nakano, M. Kai, M. Ohno, Y. Ohjura, High-performance liquid chromatography of N-terminal tyrosine-containing oligopeptides by pre-column fluorescence derivatization with hydroxylamine, cobalt(II) and borate reagents, J. of Chromatogr. A 411 (1987) 305–311.

[34] K. Plankensteiner, A. Righi, B.M. Rode, Glycine and Diglycine as Possible Catalytic Factors in the Prebiotic Evolution of Peptides, Orig. of Life and Evol. of Biosph 32 (2002) 225–236.

[35] J.G. Nery, G. Bolbach, I. Weissbuch, M. Lahav, Homochiral Oligopeptides Generated by Induced "Mirror Symmetry Breaking" Lattice-Controlled Polymerizations in Racemic Crystals of Phenylalanine N-Carboxyanhydride, Chem. A Eur. J. 11 (2005) 3039–3048.

[36] X. Li, P. Fan, M. Zang, J. Xing, Rapid Determination of Oligopeptides and Amino Acids in Soybean Protein Hydrolysates using High-Resolution Mass Spectrometry, Phytochem. Anal. 26 (2015) 15–22.

[37] S. Sforza, G. Aquino, V. Cavatorta, G. Galaverna, G. Mucchetti, A. Dossena, R. Marchelli, Proteolytic oligopeptides as molecular markers for the presence of cows' milk in fresh cheeses derived from sheep milk, Int. Dairy J. 18 (2008) 1072–1076.

[38] T. Otake, T. Taniguchi, Y. Furukawa, F. Kawamura, H. Nakazawa, T. Kakegawa, Stability of Amino Acids and Their Oligomerization Under High-Pressure Conditions: Implications for Prebiotic Chemistry, Astrobiology 11 (2011) 799–813.

[39] U. Shanker, B. Bhushan, G. Bhattacharjee, Kamaluddin, Oligomerization of Glycine and Alanine Catalyzed by Iron Oxides: Implications for Prebiotic Chemistry, Orig. of Life and Evol. of Biosph. 42 (2012) 31–45.

[40] J. You, X. Fan, H.E. Wang, G. Wang, J.X. Su, C.L. Zhou, High-Performance Liquid Chromatographic Determination of Amino Acids and Oligopeptides by Pre-column Fluorescence Derivatization with 9-Fluorenyl-methoxy Carbonyl Succinimide, J. of Liq. Chromatogr. and Relat. Technol. 21 (1998) 2103–2115.

[41] H. Wang, J. Li, T.-X. Yang, H.-S. Zhang, N-Hydroxysuccinimidy-Fluorescein-O-Acetate for Precolumn Fluorescence Derivatization of Amino Acids and Oligopeptides in Liquid Chromatography, J. of Chromatogr. Sci. 39 (2001) 365–369.

[42] Y. Zubavichus, M. Zharnikov, A. Schaporenko, M. Grunze, NEXAFS study of glycine and glycine-based oligopeptides, J. of Electron Spectrosc. and Relat. Phenom. 134 (2004) 25–33.

[43] J.G. Forsythe, A.S. Petrov, W.C. Millar, S.-S. Yu, R. Krishnamurthy, M.A. Grover, N.V. Hud, F.M. Fernández, Surveying the sequence diversity of model prebiotic peptides by mass spectrometry, Proc. of the Natl. Acad. of Sci. U.S.A. 114 (2017) E7652–E7659.

[44] A. Brack, K.W. Ehler, L.E. Orgel, N,N'-carbonyldiimidazole-induced diketopiperazine formation in aqueous solution in the presence of adenosine-5'-monophosphate, J. of Mol. Evol. 8 (1976) 307–310.

[45] A.L. Weber, L.E. Orgel, The formation of peptides from the 2'(3')-glycyl ester of a nucleotide, J. of Mol. Evol. 11 (1978) 189–198.

[46] A.L. Weber, L.E. Orgel, The formation of dipeptides from amino acids and the 2'(3')-glycyl ester of an adenylate, J. of Mol. Evol. 13 (1979) 185–191.

[47] V.R. Klement, G. Biberacher, V. Hille, Contributions to the knowledge of monoamido and diamido phosphoric acid, Z. für Anorg. und Allg. Chem. 289 (1957) 80–89.

[48] M. Watanabe, S. Sato, The synthesis and thermal behavior of sodium phosphorodiamidate, J. of Mater. Sci. 21 (1986) 2623–2627.

[49] A.S. Burton, J.C. Stern, J.E. Elsila, D.P. Glavin, J.P. Dworkin, Understanding prebiotic chemistry through the analysis of extraterrestrial amino acids and nucleobases in meteorites, Chem. Soc. Rev 41 (2012) 5459–5472.

[50] S.A. Cohen, D.P. Michaud, Synthesis of a Fluorescent Derivatizing Reagent, 6-Aminoquinolyl-N-Hydroxysuccinimidyl Carbamate, and Its Application for the Analysis of Hydrolysate Amino Acids via High-Performance Liquid Chromatography, Anal. Biochem. 211 (1993) 279–287.

[51] F. Lai, A. Mayer, T. Sheehan, Matrix effects in the derivatization of amino acids with 9-fluorenylmethyl chloroformate and phenylisothiocyanate, BioTechniques 11 (1991) 23–244.

[52] D.P. Glavin, J.L. Bada, Isolation of Amino Acids from Natural Samples Using Sublimation, Anal. Chem. 70 (1998) 3119–3122.

[53] M.C. García Alvarez-Coque, M.J. Medina Hernández, R.M. Villanueva Camanas, C. Mongay Fernández, Formation and instability of o-phthalaldehyde derivatives of amino acids, Anal. Biochem. 178 (1989) 1–7.

[54] K. Kawamura, H. Takeya, T. Kushibe, Y. Koizumi, Mineral-Enhanced Hydrothermal Oligopeptide Formation at the Second Time Scale, Astrobiol 11 (2011) 461–469.

[55] M. Rodriguez-Garcia, A.J. Surman, G.J. Cooper, I. Suárez-Marina, Z. Hosni, M.P. Lee, L. Cronin, Formation of oligopeptides in high yield under simple programmable conditions, Nature Commun 6 (2015) 8385, doi:10.1038/ncomms9385.

[56] J.M. You, G.H. Xie, H.E. Wang, J.X. Su, C.L. Zhou, HPLC of Amino Acids and Oligopeptides by Pre-Column Fluorescence Derivatization with N-Hydroxysuccinimidyl-α-(9-phenanthrene)-acetate, Chromatographia 46 (1997) 245–250.

[57] R. Zhu, W.T. Kok, Postcolumn derivatization of peptides with fluorescamine in capillary electrophoresis, J. of Chromatogr. A 814 (1998) 213–221.

[58] W. Wang, Z. Wang, X. Lin, Z.W. Wang, F.F. Fu, Simultaneous analysis of seven oligopeptides in microbial fuel cell by micro-fluidic chip with reflux injection mode, Talanta 100 (2012) 338–343.

[59] T.D. Campbell, R. Febrian, H.E. Kleinschmidt, K.A. Smith, P.J. Bracher, Quantitative Analysis of Glycine Oligomerization by Ion-Pair Chromatography, ACS Omega 4 (2019) 12745–12752.
[60] I. Hamrníková, I. Mikšík, M. Uhrová, Z. Deyl, Ultraviolet detector response of glycine and alanine homopeptides: Some specific features in capillary electrophoresis, Anal. Chim. Acta 372 (1998) 257–272.
[61] H. Sugahara, K. Mimura, Glycine oligomerization up to triglycine by shock experiments simulating comet impacts, Geochem. J. 48 (2014) 51–62.
[62] C. Fujimoto, A. Shinozaki, K. Mimura, T. Nishida, H. Gotou, K. Komatsu, H. Kagi, Pressure-induced oligomerization of alanine at 25 °C, Chem. Commun. 51 (2015) 13358–13361.
[63] C.J. Peacock, G. Nickless, The Dissociation Constants of some Phosphorus(V) Acids, Z. für Naturforschung 24 (1969) 245–247.
[64] R.B. Martin, Free energies and equilibria of peptide bond hydrolysis and formation, Biopolymers 45 (1998) 351–353.
[65] I. Mamajanov, P.J. MacDonald, J. Ying, D.M. Duncanson, G.R. Dowdy, C.A. Walker, A.E. Engelhart, F.M. Fernández, M.A. Grover, N.V. Hud, F.J. Schork, Ester Formation and Hydrolysis during Wet-Dry Cycles: Generation of Far-from-Equilibrium Polymers in a Model Prebiotic Reaction, Macromolecules 47 (2014) 1334–1343.
[66] N. Lahav, D. White, S. Chang, Peptide formation in the prebiotic era: thermal condensation of glycine in fluctuating clay environments, Science 201 (1978) 67–69.
[67] H. Le Son, Y. Suwannachot, J. Bujdak, B.M. Rode, Salt-induced peptide formation from amino acids in the presence of clays and related catalysts, Inorg. Chim. Acta 272 (1998) 89–94.
[68] J.E. Purdie, N.L. Benoiton, Piperazinedione formation from esters of dipeptides containing glycine, alanine, and sarcosine: the kinetics in aqueous solution, J. of the Chem. Soc., Perkin Trans. 2 (14) (1973) 1845–1852, doi:10.1039/P29730001845.
[69] S. Steinberg, J.L. Bada, Diketopiperazine Formation During Investigations of Amino Acid Racemization in Dipeptides, Science 213 (1981) 544–545.
[70] S.M. Gaines, J.L. Bada, Aspartame Decomposition and Epimerization in the Diketopiperazine and Dipeptide Products as a Function of pH and Temperature, J. of Org. Chem 53 (1988) 2757–2764.
[71] K. Dose, J. Hartmann, M.C. Brand, Formation of specific amino acid sequences during carbodiimide-mediated condensation of amino acids in aqueous solution, Biosystems 15 (1982) 195–200.
[72] J.P. Greenstein, M. Winitz, Chemistry of the Amino Acids, 2, John Wiley & Sons, Inc., New York, 1961.
[73] L.E. Orgel, The origin of polynucleotide-directed protein synthesis, J. of Mol. Evol. 29 (1989) 465–474.
[74] R. Liu, L.E. Orgel, Polymerization of β-amino Acids in Aqueous Solution, Orig. of Life and Evol. of Biosph. 28 (1998) 47–60.
[75] J.M. Edmond, K.L. Von Damm, R.E. McDuff, C.I. Measures, Chemistry of hot springs on the East Pacific Rise and their effluent dispersal, Nature 297 (1982) 187–191.
[76] R. Stribling, S.L. Miller, Energy yields for hydrogen cyanide and formaldehyde syntheses: The hcn and amino acid concentrations in the primitive ocean, Orig, of Life 17 (1987) 261–273.
[77] J.L. Bada, A. Lazcano, Some Like It Hot, But Not the First Biomolecules, Science 296 (2002) 1982–1983.
[78] J.L. Bada, New insights into prebiotic chemistry from Stanley Miller's spark discharge experiments, Chem. Soc. Rev. 42 (2013) 2186–2196.
[79] S. Miyakawa, H.J. Cleaves, S.L. Miller, The Cold Origin of Life: A. Implications Based On The Hydrolytic Stabilities Of Hydrogen Cyanide And Formamide, Orig. of Life and Evol. of Biosph. 32 (2002) 195–208.
[80] J.D. Toner, D.C. Catling, Alkaline lake settings for concentrated prebiotic cyanide and the origin of life, Geochim. et Cosmochim. Acta 260 (2019) 124–132.
[81] D.P. Glavin, M.P. Callahan, J.P. Dworkin, J.E. Elsila, The effects of parent body processes on amino acids in carbonaceous chondrites, Meteorit. & Planet. Sci. 45 (2010) 1948–1972.
[82] M.M.B. Ribeiro, I.D. Serrano, S.S. Santos, Turning Endogenous Peptides into New Analgesics: The Example of Kyotorphin Derivatives, in: M. Castanho, N.C. Santos (Eds.), Peptide Drug Discovery and Development: Translational Research in Academia and Industry, Wiley-CVH, 2011, pp. 171–188.
[83] S. Santos, I. Torcato, M.A.R.B Castanho, Biomedical Applications of Dipeptides and Tripeptides, Pept. Sci. 98 (2012) 288–293.
[84] T. Soga, M. Sugimoto, M. Honma, M. Mori, K. Igarashi, K. Kashikura, S. Ideka, A. Hirayama, T. Yamamoto, H. Yoshida, M. Otsuka, S. Tsuji, Y. Yatomi, T. Sakuragawa, H. Watanabe, K. Nihei, T. Saito, S. Kawata, M. Suematsu, Serum metabolomics reveals γ-glutamyl dipeptides as biomarkers for discrimination among different forms of liver disease, J. of Hepatol. 55 (2011) 896–905.
[85] A. Hirayama, K. Igarashi, M. Tomita, T. Soga, Development of quantitative method for determination of γ-glutamyl peptides by capillary electrophoresis tandem mass spectrometry: An efficient approach avoiding matrix effect, J. of Chromatogr. A 1369 (2014) 161–169.
[86] H. Zhuang, N. Tang, Y. Yuan, Purification and identification of antioxidant peptides from corn gluten meal, J. of Funct. Foods 5 (2013) 1810–1821.
[87] A.M. Ghribi, A. Sila, R. Przbylski, N. Nedjar-Arroume, I. Makhlouf, C. Blecker, H. Attia, P. Dhulster, A. Bougatef, S. Besbes, Purification and identification of novel antioxidant peptides from enzymatic hydrolysate of chickpea (Cicer arietinum L.) protein concentrate, J. of Funct. Foods 12 (2015) 516–525.
[88] C. Esteve, M.L. Marina, M.C. García, Novel strategy for the revalorization of olive (Olea erupaea) residues based on the extraction of bioactive peptides, Food Chem 167 (2015) 272–280.
[89] S. Uno, D. Kodama, H. Yukawa, H. Shidara, M. Akamatsu, Quantitative analysis of the relationship between structure and antioxidant activity of tripeptides, J. of Pept. Sci 26 (2020) https://doi.org/10.1002/psc3238.
[90] A. Shimoyama, R. Ogasawara, Dipeptides and Diketopiperazines in the Yamato-791198 and Murchison Carbonaceous Chondrites, Orig. of Life and Evol. of Biosph 32 (2002) 165–179.
[91] P. Schmitt-Kopplin, Z. Gabelica, R.D. Gougeon, A. Fekete, B. Kanawati, M. Harir, I. Gebefuegi, G. Eckel, N. Hertkorn, High molecular diversity of extraterrestrial organic matter in Murchison meteorite revealed 40 years after its fall, Proc. of the Natl. Acad. of Sci. U.S.A 107 (2010) 2763–2768.
[92] S. Pizzarello, X. Feng, S. Epstein, J.R. Cronin, Isotopic analyses of nitrogenous compounds from the Murchison meteorite: ammonia, amines, amino acids, and polar hydrocarbons, Geochim. et Cosmochim. Acta 58 (1994) 5579–5587.

SUPPLEMENTARY MATERIAL

A Sensitive Quantitative Analysis of Abiotically Synthesized Short Homopeptides using Ultraperformance Liquid Chromatography and Time-of-Flight Mass Spectrometry

Eric T. Parker [a], Megha Karki [b, 1], Daniel P. Glavin [a], Jason P. Dworkin [a, **], Ramanarayanan Krishnamurthy [b,*]

[a]NASA Goddard Space Flight Center, Solar System Exploration Division, 8800 Greenbelt Road, Greenbelt, MD 20771, U.S.A.;
[b]Department of Chemistry, Scripps Research, 10550 North Torrey Pines Road, La Jolla, CA 92037, U.S.A.
[1]Present Address: Singular Genomics, 10931 North Torrey Pines Road Suite #100, La Jolla, CA 92037, U.S.A.

Corresponding Author:
*Ramanarayanan Krishnamurthy, Department of Chemistry, Scripps Research, 10550 North Torrey Pines Road, La Jolla, CA 92037, U.S.A.; phone: 1-858-784-8520; fax: 1-858-784-9573; email: rkrishna@scripps.edu

Co-Corresponding Author:
**Jason P. Dworkin, NASA Goddard Space Flight Center, Solar System Exploration Division, 8800 Greenbelt Road, Greenbelt, MD 20771, U.S.A.; phone: 1-301-286-8631; fax: 1-301-286-1683; email: jason.p.dworkin@nasa.gov

Supplementary Material

1. Materials and methods

1.1. Chemicals and reagents

Four reagents were used to enable pre-column derivatization of samples and standards. These four reagents were: 1) AccQ·Tag Ultra borate buffer, 2) AccQ·Tag Ultra reagent powder, 3) AccQ·Tag Ultra reagent diluent, and 4) AccQ·Tag derivatization agent**.** Reagents 1) – 3) were purchased from Waters Corporation. Reagent 4) was prepared by mixing 1 mL of reagent 3) with reagent 2). Once formed, reagent 4) was then vortexed for 10 seconds and heated for 15 minutes on top of a heating block set at 55 °C, until the powder fully dissolved, at which point, reagent 4) was ready for use as the derivatization agent as detailed in §2.2 of the main text.

Four eluents were used during analysis by UPLC-FD/ToF-MS: A) AccQ·Tag A buffer, B) AccQ·Tag B buffer, C) strong wash, and D) weak wash. Eluent A) was prepared by mixing 100 mL of AccQ·Tag Eluent A Concentrate, which was purchased from Waters Corporation, with 900 mL of Millipore ultrapure water. Eluent B) was purchased directly from Waters Corporation. Eluent C) was prepared by mixing 700 mL of HPLC grade acetonitrile with 300 mL of ultrapure water. Eluent D) was prepared by mixing 900 mL of ultrapure water with 100 mL of HPLC grade acetonitrile. Eluents A) and B) were used to perform chromatography, while eluents C) and D) were used to clean the chromatography pump.

A 0.5 M aqueous solution of sodium formate was used for daily calibrations of the ToF-MS, and real-time lock mass corrections were executed using a 200 $\mu g\ L^{-1}$ solution of leucine enkephalin. Both the 0.5 M sodium formate solution and the 200 $\mu g\ L^{-1}$ leucine enkephalin solution were prepared as described elsewhere [S1].

1.2. Method development

Chromatographic separation of target analytes was preceded by pre-column derivatization using the AccQ·Tag derivatization agent. The primary amino group of an amino acid or peptide reacted with the ester carbonyl of the derivatization agent to form a new amide bond (Figure S1), and in doing so, the target analytes were converted into a derivative with fluorescent properties. Target analyte derivatives were subsequently detected by both the FD and the ToF-MS, as detailed in §2.2 of the main text.

1.3. Analytical figures of merit

Following the development of the new analytical technique, an analytical figures of merit experiment was performed for both the FD and the ToF-MS detectors. The purpose of the analytical figures of merit experiments was to assess the quantitative accuracy and precision of the newly developed analytical technique. The analytical figures of merit experiments were performed by constructing calibration curves, produced by performing triplicate analyses of a mixed standard composed of target amino acids and homopeptides. Ten serial dilutions were generated for this experiment to obtain calibration curves across a range of 10 different analyte concentrations: 1.5 nM, 5.0 nM, 15.0 nM, 50.0 nM, 150.0 nM, 500.0 nM, 1.5 μM, 5.0 μM, 15.0 μM, and 45.0 μM.

Analytical figures of merit were obtained by performing linear regression analyses, which were executed by plotting observed standard analyte peak areas vs. known standard analyte concentrations. When doing this, it was determined that the observed analyte peak area standard deviations increased proportionally to known analyte concentrations, demonstrating the heteroscedastic nature of the acquired calibration data. Consequently, a weighted linear

regression analysis was implemented to account for heteroscedasticity in the calibration data [S3-S5]. To perform a weighted linear regression, weights (w_i) were applied:

$$\boldsymbol{w_i = \frac{s_i^{-2}}{\sum_i^n s_i^{-2}/n}} \tag{S1}$$

In equation (S1), n is the number of standard concentrations that make up the calibration curve and s_i is the standard deviation of the peak area triplicate measurements. After their application, the weights were used to determine weighted centroid coordinates ($\bar{x}_w, \bar{y}_w$):

$$\boldsymbol{\bar{x}_w = \frac{\sum_i^n w_i x_i}{n}} \tag{S2}$$

$$\boldsymbol{\bar{y}_w = \frac{\sum_i^n w_i y_i}{n}} \tag{S3}$$

In equation (S2), x_i is the analyte concentration, and in equation (S3), y_i is the observed peak area associated with x_i. Once obtained, weighted centroid coordinates were used to help calculate the weighted slope (b_w):

$$\boldsymbol{b_w = \frac{\sum_i^n w_i x_i y_i - n\bar{x}_w\bar{y}_w}{\sum_i^n w_i x_i^2 - n\bar{x}_w^2}} \tag{S4}$$

and the weighted y-intercept (a_w):

$$\boldsymbol{a_w = \bar{y}_w - b_w\bar{x}_w} \tag{S5}$$

Using the algebraic form of the general equation of a weighted straight line:

$$\boldsymbol{y_i = a_w + b_w x_i} \tag{S6}$$

the $\hat{y}_i$ component of the y-residuals ($y_i - \hat{y}_i$) can be calculated using the following equation:

$$\boldsymbol{\hat{y}_i = a_w + b_w x_i} \tag{S7}$$

when using the analyte concentration (x_i), the weighted slope (b_w, from equation (S4)), and the weighted y-intercept (a_w, from equation (S5)).

Next, the weighted, random error in the y-direction ($s_{(y/x)w}$) was obtained using:

$$\boldsymbol{s_{(y/x)w}} = \sqrt{\frac{\sum_i^n \boldsymbol{w_i(y_i - \hat{y}_i)^2}}{\boldsymbol{n-2}}} \tag{S8}$$

Finally, limit of detection (LOD) and limit of quantitation (LOQ) values for each analyte, using both detectors, were calculated as $3s_{(y/x)w}$ and $10s_{(y/x)w}$, respectively. The $3s_{(y/x)w}$ and $10s_{(y/x)w}$ values are an estimation of LOD and LOQ based on observed signal intensities. These LOD and LOQ values were then converted into their respective molar concentrations (x_i) by insertion into equation (S6) as y_i, along with inserting the calculated values for b_w and a_w into equation (S6).

The uncertainty estimates of the weighted slope are confidence intervals, which were calculated by executing a two-tailed t-test. First, the weighted standard deviations for the slope, s_{b_w}, were calculated as:

$$\boldsymbol{s_{b_w}} = \left[\frac{\boldsymbol{n}\left[\boldsymbol{s_{(y/x)w}}\right]^2}{(\boldsymbol{n}[\sum_i^n \boldsymbol{w_i x_i^2}] - [\sum_i^n \boldsymbol{w_i x_i}]^2)}\right]^{1/2} \tag{S9}$$

After the value of s_{b_w} was obtained, the confidence interval was calculated as the product of the tabulated t-value at a 95% confidence level (α= 0.05) with $n-2$ degrees of freedom and the value for s_{b_w}.

2. Results and discussion

2.1. Method development

The chromatographic approach developed in this study produced broad peaks that eluted first, followed by narrow, sharp peaks that eluted later. The reason for this observed difference in peak shape is due to the change in eluent composition during the course of the chromatographic run. When the first peaks eluted from the column, the eluent composition is <10% organic mobile phase. The Gly-based species that eluted from the column first eluted more slowly in such a strongly aqueous buffer composition, leading to relatively broad peaks (peaks 1 – 6, Figure 1). The later eluting peaks elute faster due to the greater organic eluent composition (~15%) near the end of the run, causing the sharper appearance of these later peaks.

During chromatographic optimization, an effort was made to increase the sharpness of the Gly-based peaks that eluted first. The organic composition of the eluent was increased at the time the first compounds eluted; however, it was observed that doing so caused later peaks to coelute, thereby compromising the chromatographic resolution of subsequent peaks. As a result, it was determined that the gradient described in §2.2 of the main text, which produced relatively broad peaks that eluted first and sharper peaks that eluted later (Figure 1) was acceptable because under this configuration, the chromatographic resolution of target analytes was largely preserved. A detailed accounting of resultant detection metrics is shown in Table S1.

2.2. Analytical figures of merit

The analytical figures of merit experiments resulted in the determination of the LOD, LOQ, sensitivity, and linear range values of each detector used in the newly developed method, with respect to each individual analyte targeted in this study. Table S2 displays the analytical figures of merit for the FD. The sensitivity of the FD to each analyte was relatively similar,

approximately within a factor of 2. The FD coefficient of determinations with respect to changes in analyte concentrations were > 0.999 for all target analytes, spanning a range from slightly less than 3 orders of magnitude at the minimum (Gly_2), to more than 3 orders of magnitude at the maximum (Ala_4). The FD LOD values for all analytes were below 100 nM, with the largest LOD being for Gly_2, at 86.50 nM, and the lowest LOD being for Ala_4, at 10.01 nM. The FD LOQ values for all analytes were below 500 nM, with the largest LOQ being associated with Glu, at 429.08 nM, and the lowest LOQ being associated with Ala_4, at 24.82 nM. Also included in Table S2, are the LOD and LOQ values converted from nM to femtomoles (fmol) on column, after taking into account the injection volume and dilution effects from the derivatization reaction. The FD LOD values, in terms of femtomoles on column, spanned a range of 2.00 fmol – 17.30 fmol. Similarly, the FD LOQ values, in terms of femtomoles on column, spanned a range of 4.96 fmol – 85.82 fmol.

Table S3 displays the analytical figures of merit for the ToF-MS. The sensitivity of the ToF-MS to each analyte was as low as 0.08 nM^{-1} for Asp_4, and as high as 2.52 nM^{-1} for Ala_5. The ToF-MS coefficient of determinations with respect to changes in analyte concentrations were > 0.996 for all target analytes, spanning a range from just under 3 orders of magnitude at the minimum (Gly), to more than 4 orders of magnitude at the maximum (Ala_3). The ToF-MS LOD values for all analytes were below 50 nM, except for Gly (53.83 nM). The lowest ToF-MS LOD was for Ala_3, at 1.75 nM. The ToF-MS LOQ values for most analytes were below 100 nM, except for Gly (280.15 nM), Ala (161.95 nM), and Asp (140.12 nM). The lowest ToF-MS LOQ was for Ala_3, at 5.30 nM. Also included in Table S3, are the LOD and LOQ values converted from nM to femtomoles on column, as described above. The ToF-MS LOD, in terms of

femtomoles on column, spanned a range of 0.35 fmol – 10.77 fmol. Similarly, the ToF-MS LOQ values, in terms of femtomoles on column, spanned a range of 1.06 fmol – 56.03 fmol.

The analytical figures of merit for the FD (Table S2) and the ToF-MS (Table S3) allow for a comparison between the two types of detectors used in the method developed here. It can be seen that the FD is consistently more sensitive than the ToF-MS. However, the LOD and LOQ values for the FD are both generally greater than that observed for the ToF-MS. To understand the reasoning for this, it is important to keep in mind that instrumental sensitivity is defined as the instrument response to a given analyte, per unit concentration of that analyte, whereas the LOD and LOQ values are functions of the backgrounds observed by the detector for a given analyte. The FD exhibited a greater response per unit concentration of each target analyte it was exposed to, yet the background observed by the FD was greater for most analytes, than that which was observed by the ToF-MS. Consequently, the ToF-MS demonstrated a greater overall ability to limit background noise associated with most analytes than was the FD. Therefore, the ToF-MS boasted a lower LOD for 15 of the target analytes and a lower LOQ for 16 of the target analytes, than did the FD. During the evaluation of the performance of the method developed here, it can be seen that this new technique is a sensitive analytical tool that provides low LOD and LOQ values for amino acids and respective homopeptides, while using multiple detectors to identify target analytes via 3 different analytical metrics, including accurate mass measurements.

2.3. Room temperature/heating experiments

Small quantities of Gly_3 were produced by the fourth collection time (t_4 = 24 days) for room temperature and mildly heated experimental reaction solutions. The signal intensities for this analyte in both the room temperature and mildly heated experimental reaction solutions reached a maximum at t_f = 106 days (Figure S2). Gly_3 abundances are not reported here because

the analyte concentrations did not exceed the instrumental LOQ. Additionally, Gly-based homopeptides longer than trimers were not formed over the course of the 106-day experiment.

Accurate mass chromatograms demonstrate the detection of Ala_2 in the experimental reaction solutions, but the absence of Ala_2 in the experimental control solutions (Figure S3). The temporal Ala_2 formation under room temperature and mild heating conditions, is displayed in Figure S4 for both experimental control and reaction solutions. Experimental control solutions failed to generate detectable quantities of Ala_2. Experimental reaction solutions generated detectable quantities of Ala_2 by the first collection time (t_1 = 3 days) when exposed to mild heating (50 °C), but failed to generate detectable quantities of Ala_2 until after the third collection time (t_3 = 9 days) when left at room temperature. Given the disparate synthetic trends between room temperature and mild heating conditions at the onset of the experiment, it was surprising to observe that the room temperature experimental reaction solutions produced almost twice as much Ala_2 after 106 days than did the mildly heated experimental reaction solutions (Figure S4). The room temperature experimental reaction solutions produced ~77 μM of Ala_2, while the heated experimental reaction solutions produced ~40 μM of Ala_2 (Table 4). Small quantities of Ala_3 were produced in both the room temperature and heating experiments, where maximum concentrations were observed after 106 days (Figure S5) for both room temperature and mild heating conditions. Ala_3 abundances are not reported here because the analyte concentrations did not exceed the instrumental LOQ. Furthermore, Ala-based homopeptides longer than trimers were not observed over the course of the 106-day experiment.

Upon confirming that DAP successfully facilitated the oligomerization of simple amino acids, such as Gly and Ala, it was explored if DAP could facilitate amino acid oligomerization of more complex monomers, such as Asp and Glu. Under room temperature conditions, maximum

Asp_2 formation was observed after 24 days, while maximum Asp_2 formation was observed after 9 days when mild heating was applied (Table 4). While the differences between these maximum Asp_2 abundances appeared to be significant when examining accurate mass LC-MS data (Figure S6), the quantitative synthetic trends of Asp_2 over the course of the 106-day experiment appeared to be surprisingly similar for both room temperature and mild heating conditions (Figure S7). As was the case with simple amino acids, such as Gly, experimental control solutions failed to produce Asp-based peptides, confirming the necessity of DAP to induce oligomerization. Experimental reaction solutions generated detectable quantities of Asp_2 by the first collection time (t_1 = 3 days) under both room temperature and mild heating (50 °C) conditions, demonstrating the facile nature by which Asp oligomerized in the presence of DAP. However, Asp-based homopeptides longer than dimers were not formed during the experiment.

Accurate mass chromatograms of Glu_2 formation at the respective time points of maximum signal intensities for both the room temperature and mild heating experimental reaction solutions indicate that the room temperature experiments generated a greater maximum quantity of Glu_2 over the course of the 106-day experiment than did the heating experiments (Figure S8). The temporal Glu_2 formation under room temperature and mild heating conditions is displayed in Figure S9 for both experimental control and reaction solutions. Experimental control solutions failed to produce Glu-based peptides, while experimental reaction solutions produced minimal quantities (~2 μM) of Glu_2 under room temperature conditions. Glu_2 abundances formed under mild heating conditions are not reported here because under these conditions, Glu_2 was detected just over the LOD, but did not exceed the instrumental LOQ. Experimental reaction solutions generated detectable quantities of Glu_2 by the fourth collection time (t_4 = 24 days) when exposed to both room temperature and mild heating (50 °C) conditions.

Furthermore, Glu-based homopeptides longer than dimers could not be detected in either the room temperature experimental reaction solutions, or those exposed to mild heating at 50 °C. This result underscores that Glu does not oligomerize nearly as readily as the other three amino acids tested under the same experimental conditions.

2.4. Simulated environmental wet-dry cycling experiments

For the purpose of evaluating if DAP was capable of facilitating the oligomerization of peptides, in addition to amino acids, Gly_2 was used as an additional test starting reagent to determine if oligomers of Gly_2 were preferentially synthesized upon exposure to simulated environmental cycling. Under these conditions, it can be seen that in the absence of cycling (t_i), only Gly_2 is detectable (Figure S10A). However, after cycling is implemented, Gly_4 and Gly_6 are also detectable, indicating that Gly_2 was successfully oligomerized into its dimer and trimer (Figure S10B). It is worth noting that Gly_3 and Gly_5 were disproportionately not formed in this experiment; however, a small peak for Gly_3 was observed in the mass chromatogram (Figure S10B), likely due to the presence of trace amounts of Gly contaminant reacting with Gly_2 and DAP during the oligomerization reaction to form minute quantities of Gly_3. The formation of Gly_2 oligomers as a function of simulated environmental cycles is shown in Figure S10C where it can be seen that, as expected, Gly_4 was formed more prevalently than Gly_6, but that Gly_6 was still readily generated to appreciable quantities (~363 μM) after 4 cycles (Table 5). The higher abundances of Gly_4 than Gly_6 may be partially due to aqueous solubility limitations associated with Gly_6.

References

[S1] D.P. Glavin, J.E. Elsila, H.L. McLain, J.C. Aponte, E.T. Parker, J.P. Dworkin, D.H. Hill, H.C. Connolly Jr., D.S. Lauretta, Extraterrestrial amino acids and L-enantiomeric excesses in the CM2 carbonaceous chondrites Aguas Zarcas and Murchison, Meteorit. & Planet. Sci. (2020) https://doi.org/10.1111/maps.13451.

[S2] S.A. Cohen, D.P. Michaud, Synthesis of a Fluorescent Derivatizing Reagent, 6-Aminoquinolyl-N-Hydroxysuccinimidyl Carbamate, and Its Application for the Analysis of Hydrolysate Amino Acids via High-Performance Liquid Chromatography, Anal. Biochem. 211 (1993) 279-287.

[S3] K. Danzer, L.A. Currie, Guidelines for Calibration in Analytical Chemistry. Part 1. Fundamentals and Single Component Calibration, Pure and Appl. Chem. 70 (1998) 993-1014.

[S4] M.E Monge, J.J. Perez, P. Dwivedi, M. Zhou, N.A. McCarty, A.A. Stecenko, F.M. Fernández, Ion mobility and liquid chromatography/mass spectrometry strategies for exhaled breath condensate glucose quantitation in cystic fibrosis studies, Rapid Commun. in Mass Spectrom. 27 (2013) 2263-2271.

[S5] E.T. Parker, H.J. Cleaves II, J.L. Bada, F.M. Fernández, Quantitation of α-hydroxy acids in complex prebiotic mixtures via liquid chromatography/tandem mass spectrometry, Rapid Commun. in Mass Spectrom. 30 (2016) 2043-2051.

Figures

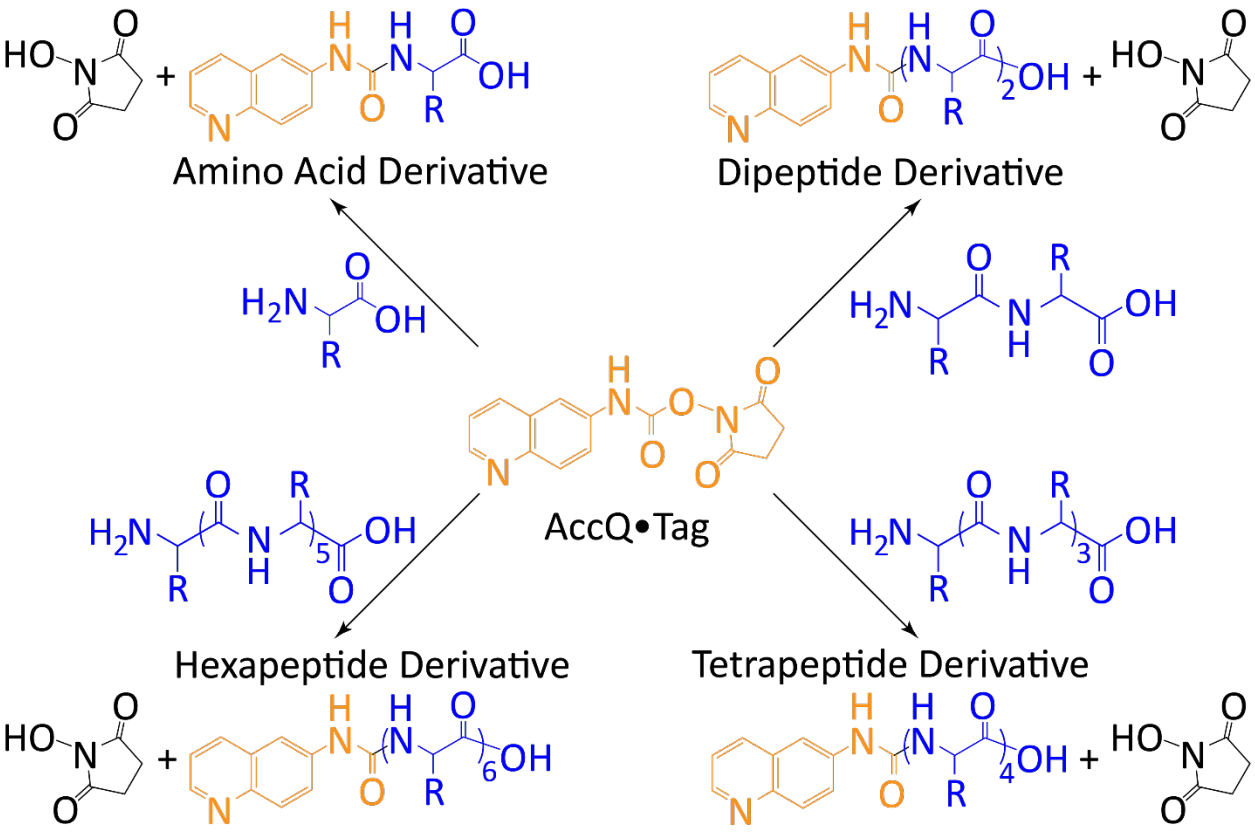

Figure S1. Schematic of AccQ·Tag derivatization reaction. This schematic gives general examples of how the AccQ·Tag derivatization agent reacts with amino acids and homopeptides to yield the derivatized target analyte that were subsequently detected and quantitated by UPLC-FD/ToF-MS. The schematic shown here is based on Cohen and Michaud [S2].

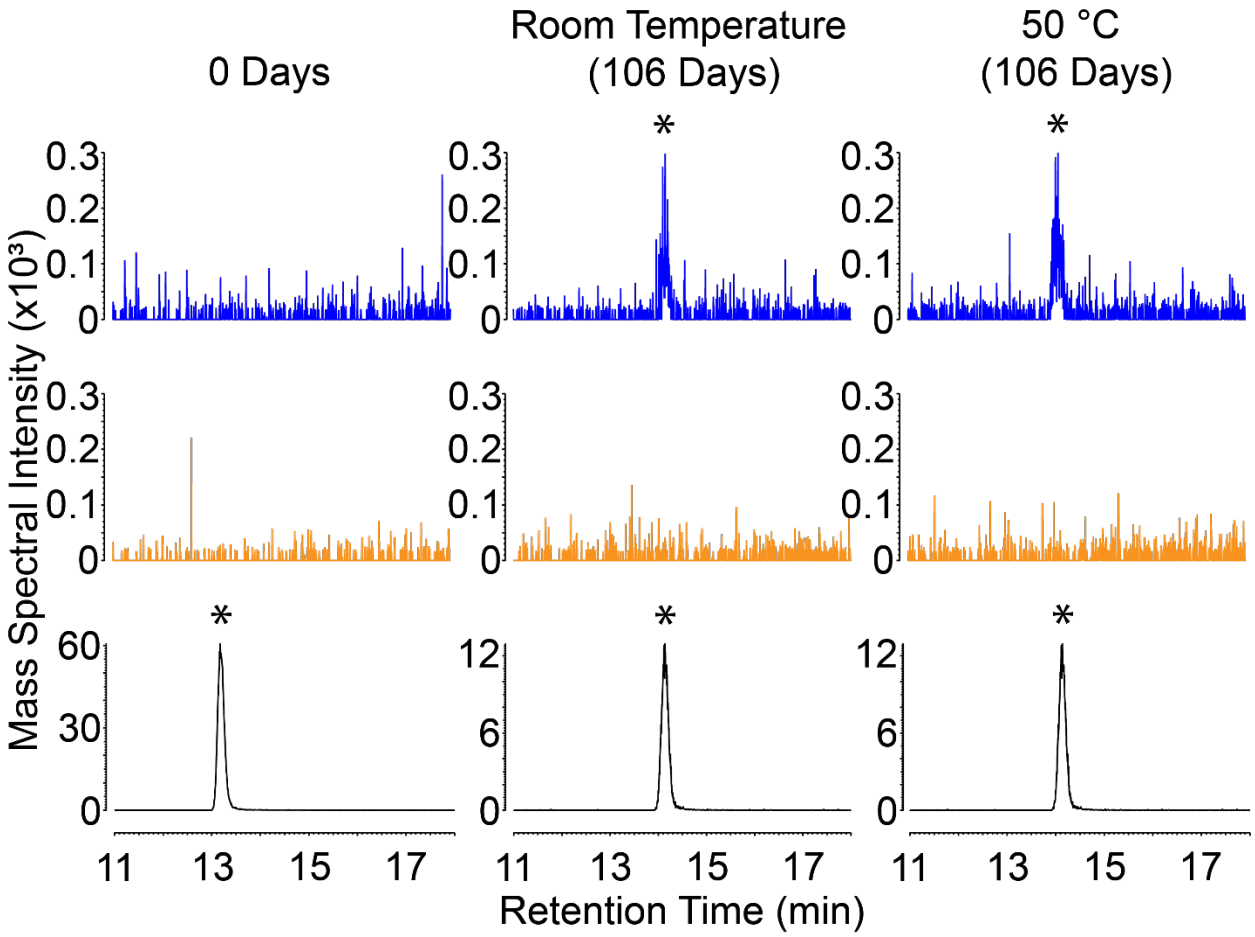

Figure S2. Gly_3 production under room temperature and mild heating conditions. Accurate mass chromatograms of a Gly_3 standard (bottom, black), reaction mixture of a solution of Gly + imidazole (middle, orange), and reaction mixture of a solution of Gly + imidazole + DAP (top, blue). Data are collected after 0 days (t_i) and 106 days (t_f) when maximum Gly_3 signal intensities were reached for both the room temperature and mild heating (50 °C) experimental reaction solutions. Accurate mass chromatograms were extracted from *m/z* 360.1308. Asterisks denote peaks that represent Gly_3. Here, min = minutes.

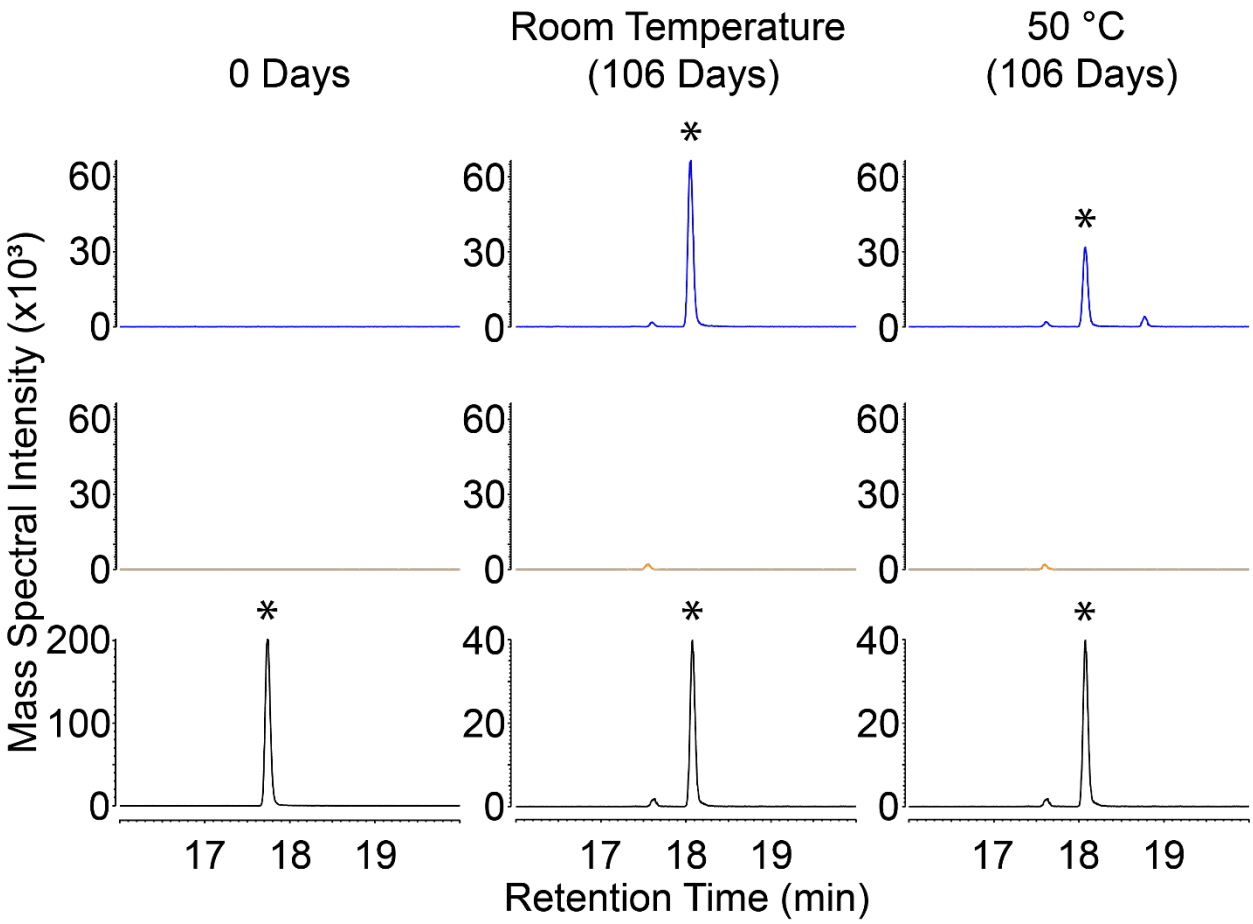

Figure S3. Ala_2 production under room temperature and mild heating conditions. Accurate mass chromatograms of an Ala_2 standard (bottom, black), reaction mixture of a solution of Ala + imidazole (middle, orange), and reaction mixture a solution of Ala + imidazole + DAP (top, blue). Data are collected after 0 days (t_i) and 106 days (t_f) when maximum Ala_2 concentrations were reached for both room temperature and mild heating (50 °C) experimental reaction solutions. Accurate mass chromatograms were extracted from *m/z* 331.1406. Asterisks denote peaks that represent Ala_2. Here, min = minutes.

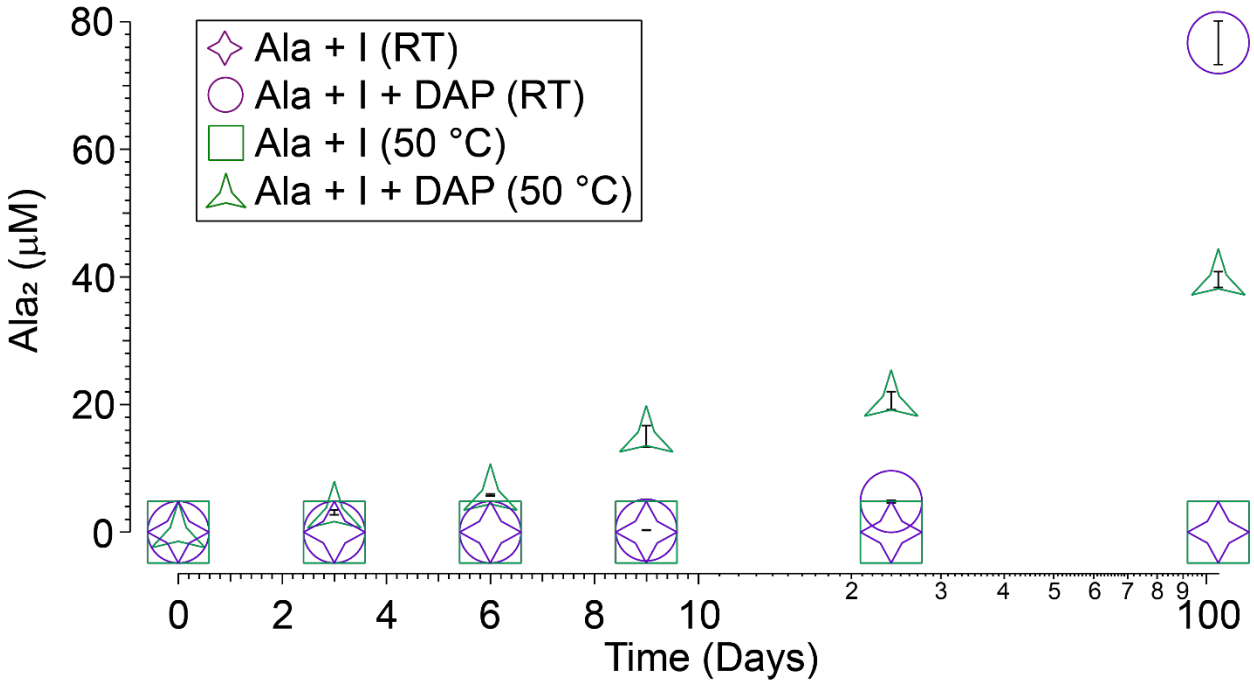

Figure S4. Temporal Ala_2 production under room temperature and mild heating conditions. Ala_2 is not synthesized in the absence of DAP, and Ala_2 synthesis was surprisingly enhanced at the end of the 106-day experiment, under room temperature conditions. Samples portrayed here were analyzed in triplicate. Uncertainties (δ_x) were determined as the standard error ($\delta_x = \sigma_x \cdot (n)^{-1/2}$), whereby the uncertainties were based on the standard deviation (σ_x) of the average value of 3 separate measurements ($n = 3$). In this figure, I = imidazole, and RT = room temperature.

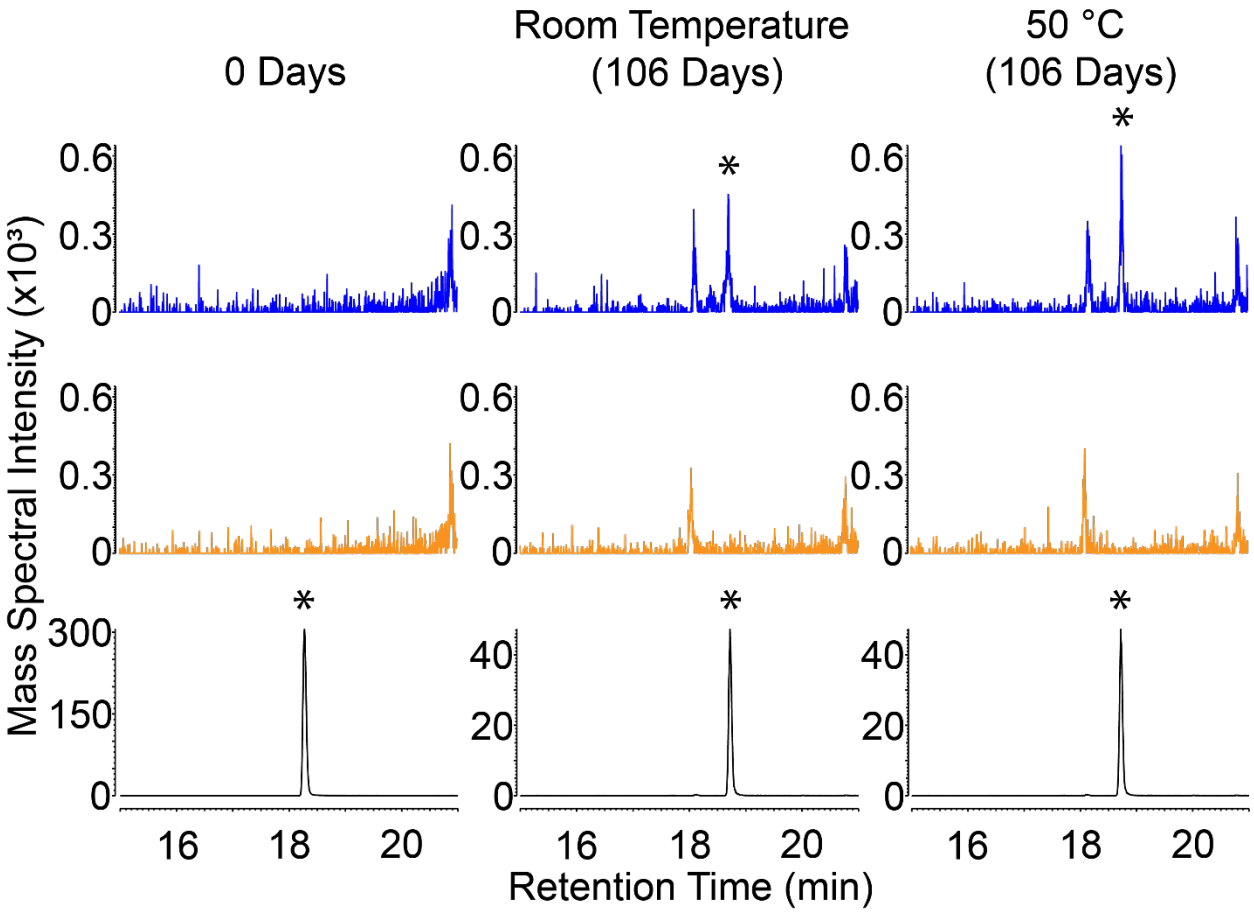

Figure S5. Ala_3 production under room temperature and mild heating conditions. Accurate mass chromatograms of an Ala_3 standard (bottom, black), reaction mixture of a solution of Ala + imidazole (middle, orange), and reaction mixture of a solution of Ala + imidazole + DAP (top, blue). Data are collected after 0 days (t_i) and 106 days (t_f) when maximum Ala_3 signal intensities were reached for both room temperature and mild heating (50 °C) experimental reaction solutions. Accurate mass chromatograms were extracted from *m/z* 402.1777. Asterisks denote peaks that represent Ala_3. Here, min = minutes.

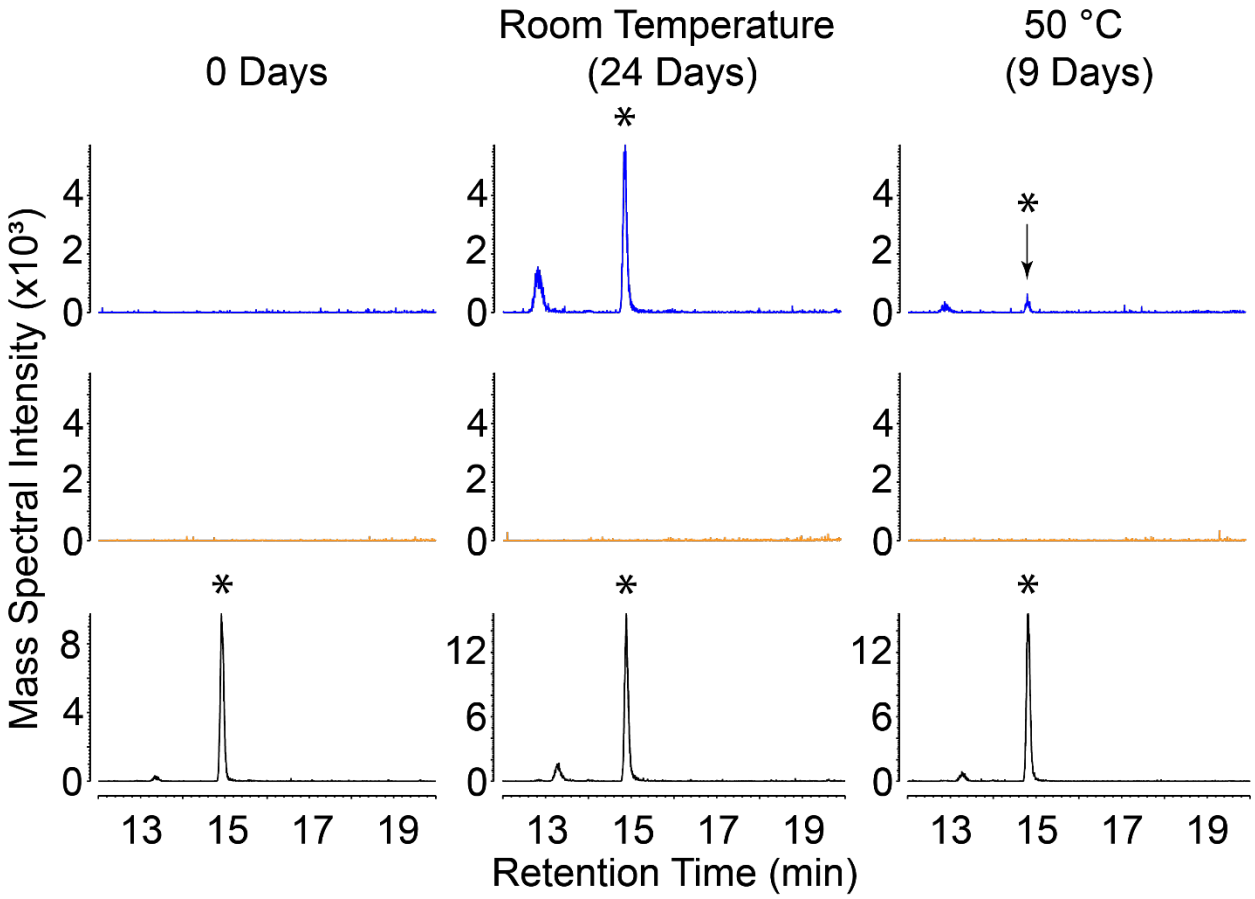

Figure S6. Asp_2 production under room temperature and mild heating conditions. Accurate mass chromatograms of an Asp_2 standard (bottom, black), reaction mixture of a solution of Asp + imidazole (middle, orange), and reaction mixture of a solution of Asp + imidazole + DAP (top, blue). Data are collected after 0 days (t_i), after 24 days (t_4) when maximum Asp_2 concentrations were reached for room temperature experimental reaction solutions, and after 9 days (t_3) when maximum Asp_2 concentrations were reached for mild heating (50 °C) experimental reaction solutions. Accurate mass chromatograms were extracted from *m/z* 419.1203. Asterisks denote peaks that represent Asp_2. Here, min = minutes.

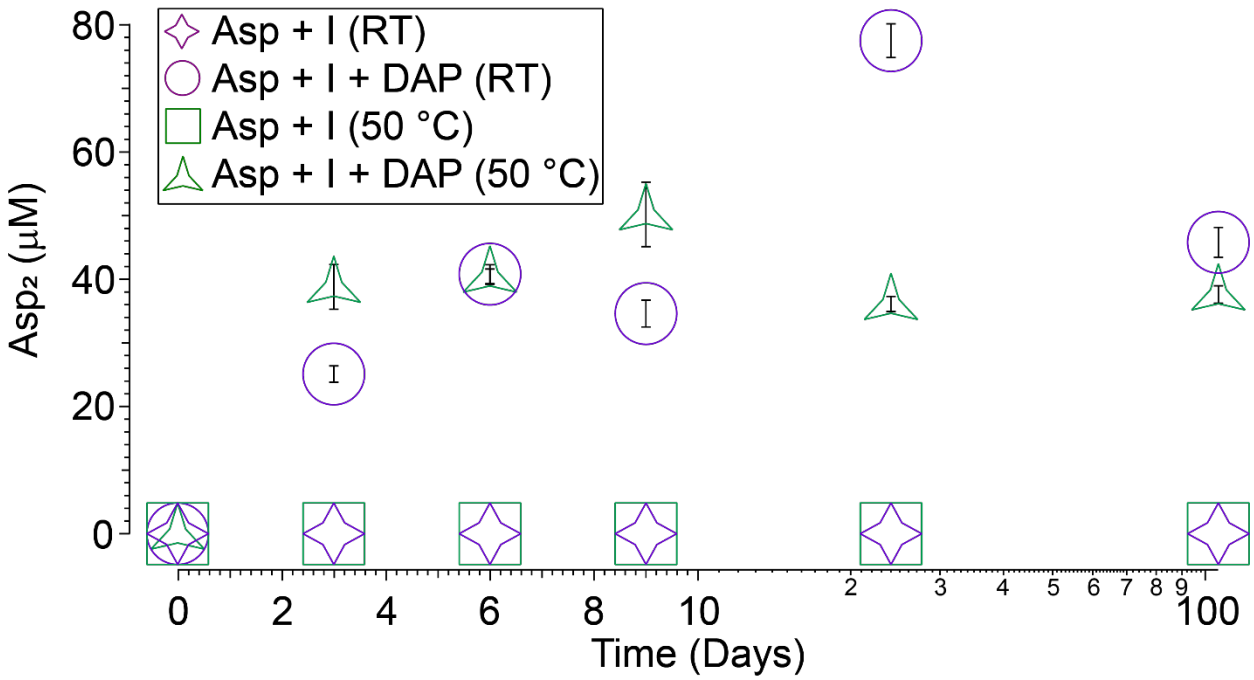

Figure S7. Temporal Asp_2 production under room temperature and mild heating conditions. Asp_2 is not synthesized in the absence of DAP, and Asp_2 synthesis is surprisingly similar between room temperature and mild heating conditions. Samples portrayed here were analyzed in triplicate. Uncertainties (δ_x) were determined as the standard error ($\delta_x = \sigma_x \cdot (n)^{-1/2}$), whereby the uncertainties were based on the standard deviation (σ_x) of the average value of 3 separate measurements ($n = 3$). In this figure, I = imidazole, and RT = room temperature.

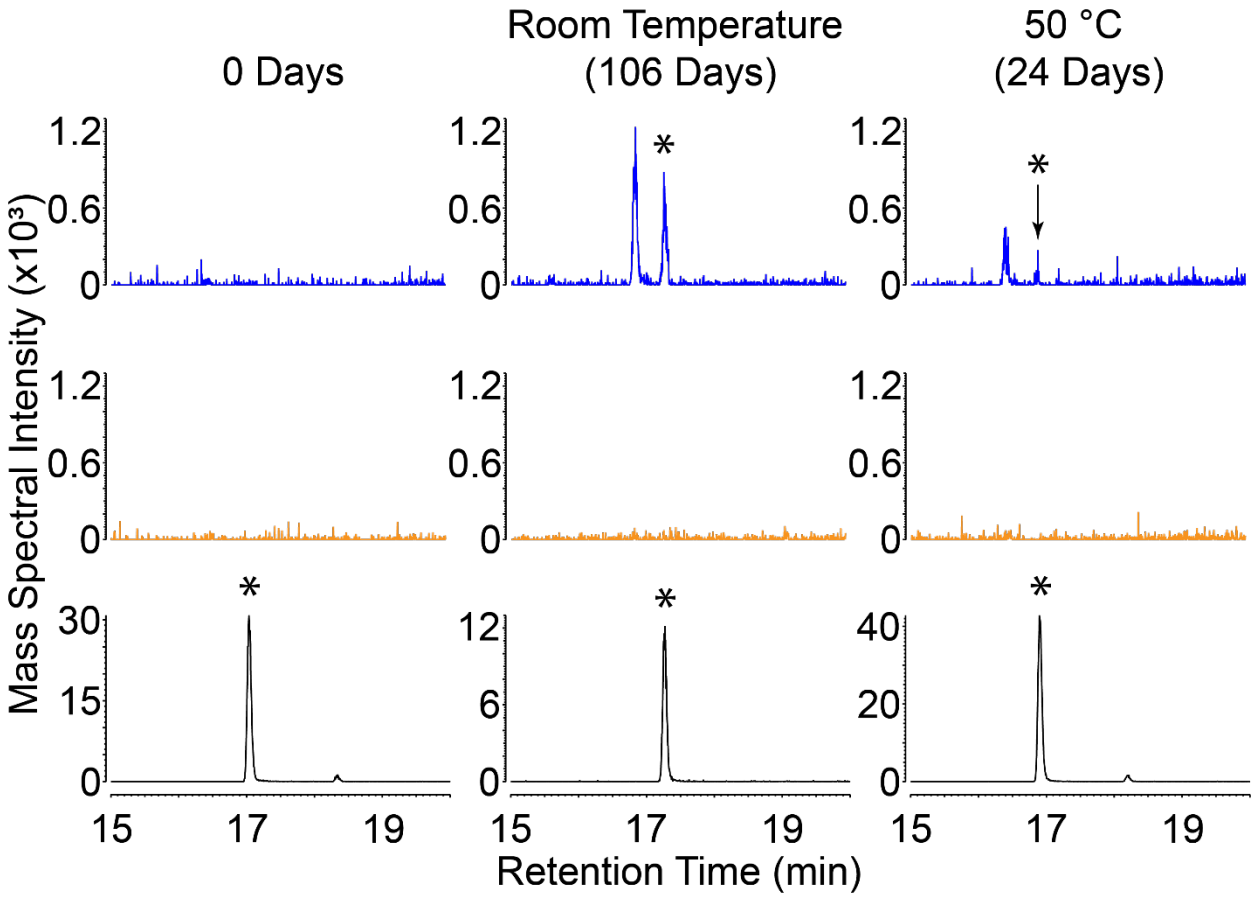

Figure S8. Glu_2 production under room temperature and mild heating conditions. Accurate mass chromatograms of a Glu_2 standard (bottom, black), reaction mixture of a solution of Glu + imidazole (middle, orange), and reaction mixture of a solution of Glu + imidazole + DAP (top, blue). Data are collected after 0 days (t_i), after 106 days (t_f) when maximum Glu_2 concentrations were reached for room temperature experimental reaction solutions, and after 24 days (t_4) when maximum Glu_2 signal intensities were reached for mild heating (50 °C) experimental reaction solutions. Accurate mass chromatograms were extracted from *m/z* 447.1516. Asterisks denote peaks that represent Glu_2. Here, min = minutes.

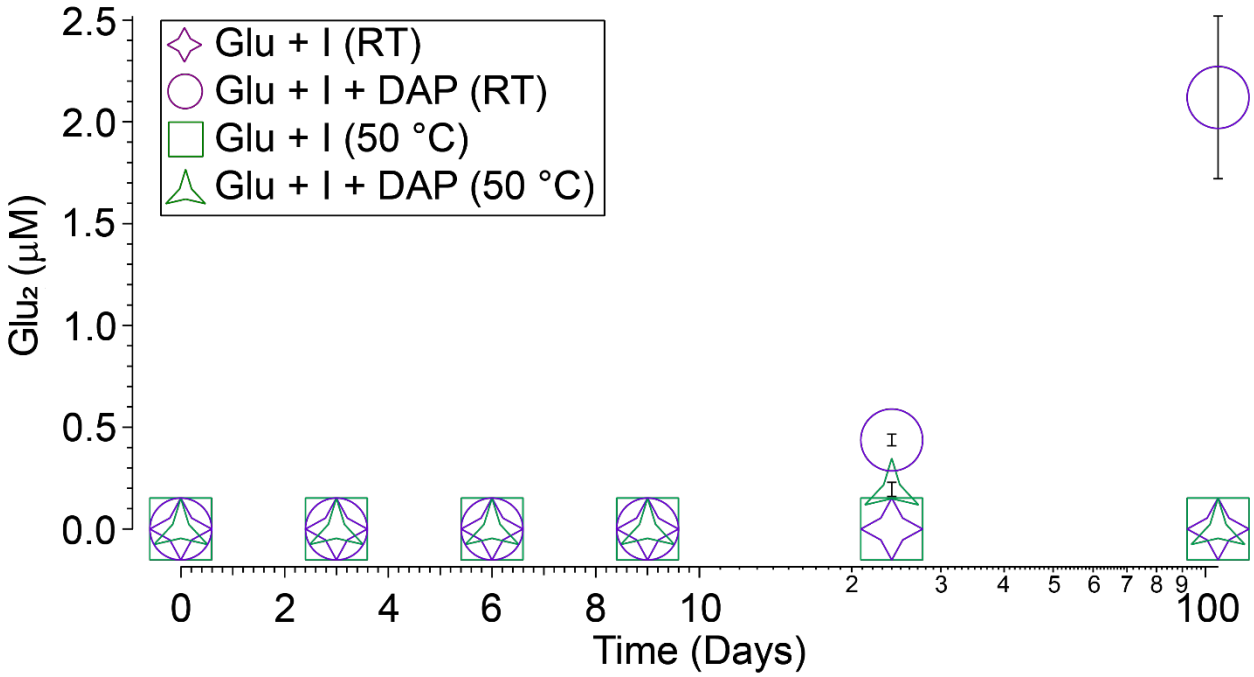

Figure S9. Temporal Glu_2 production under room temperature and mild heating conditions. Glu_2 is not synthesized in the absence of DAP. However, Glu_2 synthesis is relatively inefficient when in the presence of DAP and imidazole, possibly due to the complexity of the Glu structure compared to simpler amino acids like Gly and Ala. Measurements portrayed here were performed in triplicate, except for the t_f measurement for the Glu + imidazole + DAP room temperature experimental reaction solution, which was performed in duplicate, thus causing a larger uncertainty estimate for the corresponding measurement. Uncertainties (δ_x) were determined as the standard error ($\delta_x = \sigma_x \cdot (n)^{-1/2}$), whereby the uncertainties were based on the standard deviation (σ_x) of the average value of 2 or 3 separate measurements ($n = 2\ or\ 3$). In this figure, I = imidazole, and RT = room temperature.

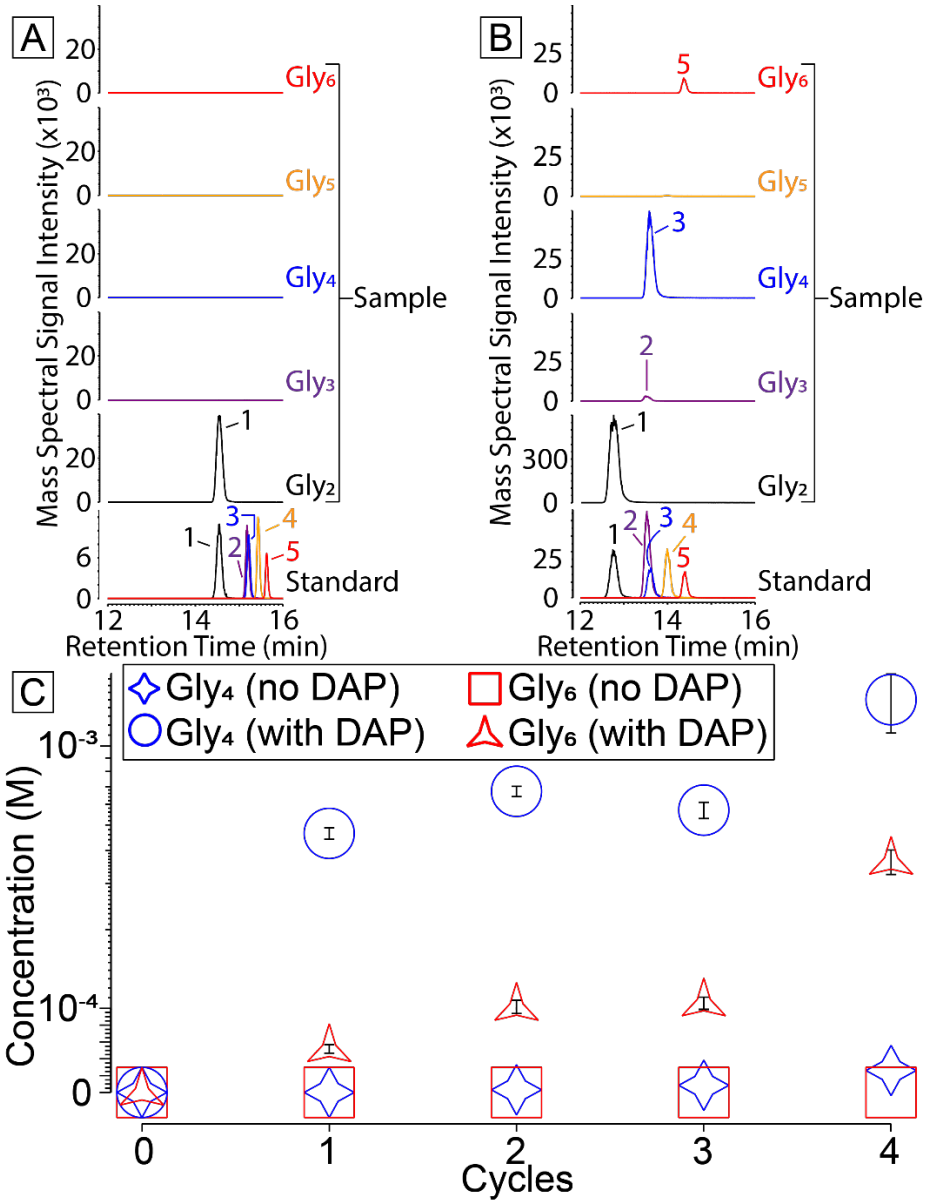

Figure S10. DAP is capable of inducing the oligomerization of peptides. A mixture of 10 mM Gly_2, 10 mM imidazole, and 10 mM DAP did not contain any oligomers of Gly_2 prior to cycling (A). However, upon cycling, it is readily observed that Gly_4 and Gly_6 were disproportionately synthesized (B). Upon completion of the cycling experiments, it can be seen that Gly_4 was consistently present at higher abundances than Gly_6 (C). Samples portrayed here were analyzed in triplicate. Uncertainties (δ_x) were determined as the standard error ($\delta_x = \sigma_x \cdot (n)^{-1/2}$), whereby the uncertainties were based on the standard deviation (σ_x) of the average value of 3 separate measurements ($n = 3$). The following *m/z* values were used to obtain the chromatograms shown in (A) and (B): Peak #1) Gly_2 = *m/z* 303.1093, Peak #2) Gly_3 = *m/z* 360.1308, Peak #3) Gly_4 = *m/z* 417.1523, Peak #4) Gly_5 = *m/z* 474.1737, and Peak #5) Gly_6 = *m/z* 531.1952. Standard chromatograms in (A) and (B) were composed by combining individual mass chromatograms of Gly-based oligomers in a mixed standard, which were run on the same days as the non-cycled sample (A) and the cycled sample (B). Here, min = minutes.

Tables

Table S1. The newly developed method provided accurate identification of target analytes. Detection metrics associated with the technique developed in this study, when exposed to a mixed standard of target amino acids and homopeptides. The data in this table was generated from the same standard run that produced the fluorescence chromatogram shown in Figure 1. Upon derivatization with AccQ·Tag, target analytes experienced a mass shift of 170 Da. Mass error was calculated as $[(mass_{theoretical} - mass_{experimental})/mass_{theoretical}]\ x\ 10^6$.

Peak Number	Analyte	LC RT (min)	MS RT (min)	$[M+H]^+$ Chemical Formula	Theoretical *m/z*	Experimental *m/z*	Mass Error (ppm)
1	Gly_2	12.22	12.29	$C_{14}H_{15}N_4O_4$	303.1093	303.1077	5.2786
2	Gly_3	13.23	13.25	$C_{16}H_{18}N_5O_5$	360.1308	360.1296	3.3321
3	Gly_4	13.23	13.34	$C_{18}H_{21}N_6O_6$	417.1523	417.1512	2.6369
4	Gly_5	13.73	13.84	$C_{20}H_{24}N_7O_7$	474.1737	474.1730	1.4763
5	Gly_6	14.17	14.26	$C_{22}H_{27}N_8O_8$	531.1952	531.1937	2.8238
6	Gly	14.59	14.68	$C_{12}H_{12}N_3O_3$	246.0879	246.0857	8.9399
7	Asp_2	14.84	14.92	$C_{18}H_{19}N_4O_8$	419.1203	419.1181	5.2491
8	Asp_3	15.40	15.49	$C_{22}H_{24}N_5O_{11}$	534.1472	534.1460	2.2466
9	Asp	15.83	15.93	$C_{14}H_{14}N_3O_5$	304.0933	304.0927	1.9731
10	Asp_4	16.21	16.30	$C_{26}H_{29}N_6O_{14}$	649.1742	649.1753	-1.6945
11	Glu	16.63	16.71	$C_{15}H_{16}N_3O_5$	318.1090	318.1082	2.5149
12	Glu_2	16.95	17.30	$C_{20}H_{23}N_4O_8$	447.1516	447.1515	0.2236
13	Glu_3	17.51	17.61	$C_{25}H_{30}N_5O_{11}$	576.1942	576.1948	-1.0413
14	Ala_2	17.65	17.74	$C_{16}H_{19}N_4O_4$	331.1406	331.1403	0.9060
15	Ala	17.95	18.04	$C_{13}H_{14}N_3O_3$	260.1035	260.1024	4.2291
16	Ala_3	18.25	18.34	$C_{19}H_{24}N_5O_5$	402.1777	402.1773	0.9946
17	Ala_4	19.17	19.26	$C_{22}H_{29}N_6O_6$	473.2149	473.2146	0.5340
18	Ala_5	19.51	19.60	$C_{25}H_{34}N_7O_7$	544.2520	544.2522	-0.3675

Table S2. Analytical figures of merit for the FD. This table reports the following analytical figures of merit for the FD: sensitivity, linear range, LOD, and LOQ.

Analyte	Regression Equation	R^2	Linear Range (nM)[a]	Sensitivity (S, nM^{-1})[b]	LOD[c] (nM)	LOD (fmol on column)	LOQ[d] (nM)	LOQ (fmol on column)
Gly	y = 1.40x + 44.59	1.0000	37.65 - 45,000	1.40 ± 0.01	37.65	7.53	203.67	40.73
Gly_2	y = 2.80x - 32.08	0.9997	86.50 - 45,000	2.80 ± 0.07	86.50	17.30	262.25	52.45
Gly_3	y = 2.36x + 17.47	0.9997	73.82 - 45,000	2.36 ± 0.05	73.82	14.76	250.19	50.04
Gly_4	y = 2.36x + 17.47	0.9997	73.82 - 45,000	2.36 ± 0.05	73.82	14.76	250.19	50.04
Gly_5	y = 1.98x + 131.56	0.9998	81.62 - 45,000	1.98 ± 0.04	81.62	16.32	379.60	75.92
Gly_6	y = 1.49x - 1.22	0.9992	27.93 - 45,000	1.49 ± 0.05	27.93	5.59	91.19	18.24
Ala	y = 1.39x - 6.94	1.0000	22.06 - 45,000	1.39 ± 0.01	22.06	4.41	79.87	15.97
Ala_2	y = 2.41x + 34.44	0.9997	50.19 - 45,000	2.41 ± 0.06	50.19	10.04	194.70	38.94
Ala_3	y = 2.54x + 27.50	0.9993	57.69 - 45,000	2.54 ± 0.03	57.69	11.54	184.90	36.98
Ala_4	y = 1.67x - 6.13	1.0000	10.01 - 45,000	1.67 ± 0.004	10.01	2.00	24.82	4.96
Ala_5	y = 3.03x + 1.45	1.0000	29.42 - 45,000	3.03 ± 0.01	29.42	5.88	99.16	19.83
Asp	y = 1.47x + 20.76	1.0000	42.47 - 45,000	1.47 ± 0.01	42.47	8.49	183.44	36.69
Asp_2	y = 2.17x - 11.23	0.9999	32.67 - 45,000	2.17 ± 0.02	32.67	6.53	96.81	19.36
Asp_3	y = 2.56x + 12.12	1.0000	83.69 - 45,000	2.56 ± 0.02	83.69	16.74	292.84	58.57
Asp_4	y = 2.25x + 26.16	0.9999	54.71 - 45,000	2.25 ± 0.04	54.71	10.94	204.99	41.00
Glu	y = 1.47x + 196.47	0.9999	35.10 - 45,000	1.47 ± 0.02	35.10	7.02	429.08	85.82
Glu_2	y = 2.39x + 61.64	0.9998	24.77 - 45,000	2.39 ± 0.03	24.77	4.95	142.83	28.57
Glu_3	y = 2.10x + 11.69	1.0000	18.89 - 45,000	2.10 ± 0.02	18.89	3.78	64.20	12.84

[a]When determining the linear range, analyte concentrations above 45,000 nM (45.0 μM) were not tested.

[b]The sensitivity of the detector to a given analyte is determined by the slope of the weighted linear regression (averaged peak area vs analyte concentration).

[c]The LOD is defined as 3 times the weighted, random error in the y-direction ($s_{(y/x)w}$). See equation (S8) for details on how to obtain the weighted, random error in the y-direction.

[d]The LOQ is defined as 10 times the weighted, random error in the y-direction ($s_{(y/x)w}$). See equation (S8) for details.

Table S3. Analytical figures of merit for the ToF-MS. This table reports the following analytical figures of merit for the ToF-MS: sensitivity, linear range, LOD, and LOQ.

Analyte	Regression Equation	R^2	Linear Range (nM)[a]	Sensitivity (S, nM^{-1})[b]	LOD[c] (nM)	LOD (fmol on column)	LOQ[d] (nM)	LOQ (fmol on column)
Gly	y = 0.65x + 25.09	0.9898	53.83 - 45,000	0.65 ± 0.09	53.83	10.77	280.15	56.03
Gly_2	y = 0.80x – 2.72	0.9981	15.39 - 45,000	0.80 ± 0.06	15.39	3.08	51.51	10.30
Gly_3	y = 0.63x – 4.39	0.9851	17.03 - 45,000	0.63 ± 0.09	17.03	3.41	40.46	8.09
Gly_4	y = 0.56x + 0.20	0.9892	25.17 - 45,000	0.56 ± 0.07	25.17	5.03	82.15	16.43
Gly_5	y = 0.51x – 0.02	0.9954	9.91 - 45,000	0.51 ± 0.03	9.91	1.98	32.91	6.58
Gly_6	y = 0.29x – 0.64	0.9975	17.20 - 45,000	0.29 ± 0.02	17.20	3.44	52.21	10.44
Ala	y = 0.79x – 1.11	0.9950	48.99 - 45,000	0.79 ± 0.06	48.99	9.80	161.95	32.39
Ala_2	y = 1.23x – 2.34	0.9932	7.12 - 45,000	1.23 ± 0.10	7.12	1.42	19.08	3.82
Ala_3	y = 1.45x – 0.33	0.9923	1.75 - 45,000	1.45 ± 0.11	1.75	0.35	5.30	1.06
Ala_4	y = 0.94x – 1.03	0.9931	4.56 - 45,000	0.94 ± 0.07	4.56	0.91	13.05	2.61
Ala_5	y = 2.52x – 0.84	0.9910	3.14 - 45,000	2.52 ± 0.21	3.14	0.63	9.74	1.95
Asp	y = 0.26x + 3.36	0.9954	31.79 - 45,000	0.26 ± 0.02	31.79	6.36	140.12	28.02
Asp_2	y = 0.14x + 0.24	0.9992	16.83 - 45,000	0.14 ± 0.004	16.83	3.37	60.29	12.06
Asp_3	y = 0.12x – 2.20	0.9991	39.66 - 45,000	0.12 ± 0.004	39.66	7.93	88.31	17.66
Asp_4	y = 0.08x – 1.66	0.9972	37.92 - 45,000	0.08 ± 0.01	37.92	7.58	77.94	15.59
Glu	y = 0.47x + 1.51	0.9940	10.65 - 45,000	0.47 ± 0.04	10.65	2.13	48.59	9.72
Glu_2	y = 0.23x + 0.33	0.9968	18.44 - 45,000	0.23 ± 0.01	18.44	3.69	64.85	12.97
Glu_3	y = 0.13x – 1.22	0.9983	22.99 - 45,000	0.13 ± 0.01	22.99	4.60	54.08	10.82

[a]When determining the linear range, analyte concentrations above 45,000 nM (45.0 μM) were not tested.

[b]The sensitivity of the detector to a given analyte is determined by the slope of the weighted linear regression (averaged peak area vs analyte concentration).

[c]The LOD is defined as 3 times the weighted, random error in the y-direction $s_{(y/x)w}$. See equation (S8) for details.

[d]The LOQ is defined as 10 times the weighted, random error in the y-direction $s_{(y/x)w}$. See equation (S8) for details.